OSR 45-11(Rev 10-22-2008)

Savannah River Site

Supplier Document Status

- [x] 1.Work May Proceed
- [ ] 2.Submit Final Document - Work may proceed
- [ ] 3.Revise and Resubmit - Work may proceed subject to Resolution of Comments
- [ ] 4.Revise and Resubmit. Work may not Proceed.
- [ ] 5.Permission to proceed is not required.

Permission to proceed does not constitute acceptance or approval of design details, calculations, test methods, analysis or materials developed or selected by the supplier, and does not relieve supplier from full compliance with contractual obligations or release of any 'holds' placed on the contract.

Document ID	Revision
SRRA021685-000008	**B**

Document Category	Date
8.0-ANALYSIS AND DESIGN REPORTS	**2017-12-13 08:23:05 AM, EST**

Reviewer
KINARD, TIFFANY BROOKE

ENVIRONMENTAL ENGINEERING AND EARTH SCIENCES
L.G. Rich Environmental Laboratory
342 Computer Court
Anderson, SC 29625

CLEMSON UNIVERSITY

Determination of constituent concentrations in field lysimeter effluents

Kathryn Peruski, Rachel Pope, Melody Maloubier, and Brian A. Powell

FY17 Final Report

SRR Project Title: SRR Technical Support Provided by Clemson University
SRR PO number: SRRA021685SR

Project PI: Brian A. Powell, bpowell@clemson.edu, 864.656.1004
Date Submitted:

Brian A. Powell — 9/28/17 — Date
Principal Investigator, Technical Reviewer

Megha Patel — 09.28.17 — Date
QA Representative, Technical Reviewer

Jeremiah Mangold, Savannah River Remediation, LLC — 11/15/2017 — Date

TABLE OF CONTENTS

Contents

LIST OF FIGURES

LIST OF TABLES

ABBREVIATIONS

BFS	Blast Furnace Slag
CDB	Citrate-Bicarbonate-Dithionite
CEC	Cation Exchange Capacity
DDI	Distilled Deionized Water
DO	Dissolved Oxygen
EDTA	Ethylenediaminetetraacetic acid
FY12Q4	Fiscal Year (YY) Quarter (Q)
HDPE	High-density Polyethylene
HNO_3	Nitric Acid
HPGe	High Purity Germanium Detector
ICP-MS	Inductively Coupled Plasma Mass Spectrometer
ID	Identification
LLD	Lower Limits of Detection
MDC	Minimum Detectable Concentration
NA	Not available; no measurement because sample volume was too small
NOM	Natural Organic Matter
NIST	National Institute of Standards and Technology
OM	Organic Matter
ppb	Parts per billion
ppm	Parts per million
PA	Performance Assessments
PVC	Polyvinyl Chloride
QA/QC	Quality Assurance and Quality Control
SRNL	Savannah River National Laboratory
SRR	Savannah River Remediation LLC
SRS	Savannah River Site
VWR	VWR Inc. (chemical and laboratory supplies)
XRD	X-Ray Diffraction

EXECUTUVE SUMMARY

This report summarizes the effluent measurements of the RadFLEx (Radiological Field Lysimeter Experiment) being run at the Savannah River Site (SRS). The facility was opened in May 2012 and effluent measurements have been performed on a quarterly basis since October 2012. A variety of radionuclide sources were present when the field lysimeter program was initiated including:

Homogenous sources (oxides or solution deposited)

- Six $Pu(V)NH_4(CO_3)$: three with natural organic matter (NOM) added and three without NOM
- Three solution deposited beta/gamma emitters, Cs-137, Co-60, Ba-133, and Eu-152
- Two NpO_2 and two NpO_2NO_3
- Six $Pu(IV)(C_2O_4)_2$ sources: three with grass on the surface and three without
- Three $Pu(III)_2(C_2O_4)_3$ sources
- Three Pu colloids (PuO_2)
- Four sediment controls with no radionuclides

Cementitious sources:

- Four radionuclide-free cementitious material (control)
- Six (3 cement, 3 grout) gamma emitters, Cs-137, Co-60, Ba-133, and Eu-152
- Four (2 cement, 2 grout) Tc-99 and I (no longer active, two have been removed and two are capped in place)

For convenience, all data from previous years have been included in this report and the data from August 2015-August 2017 have been added. Note that the Tc-99 bearing lysimeters were either capped or sampled in 2014. Therefore, there is no discussion of these lysimeters in this report.

The most relevant results observed in FY17 are as follows:

- The concentration of Pu in lysimeter effluents were on the order of 10^{-15} to 10^{-13} mol/L as determined using a pre-concentration step and ultra low level counting approach. Direct measurements using ICP-MS were at or below detection limits.
- Lysimeters containing NpO_2NO_3 sources have measurable breakthrough corresponding to 1,560 Bq and 12,795 Bq. These values correspond to 3% and 27% of the initial source activity assuming a 45.88 kBq initial source[1]. The variability in these numbers is hypothesized to be caused by heterogeneous flow of water through the lysimeter. ^{237}Np was also observed in the effluent of lysimeter 32 which contains a relatively insoluble NpO_2 source, though a significantly lower level, 1.06 Bq total, was observed in the effluent. The observation of Np in the effluent from this lysimeter implies that the NpO_2 is becoming oxidized and releasing Np(V) which can transport through the lysimeter with a relatively low K_d.
- Similar to previous years, ^{60}Co was measured in the effluent of all lysimeters containing gamma emitting radionuclides. However, the concentrations were much lower than previous sampling events. The majority of the ^{60}Co was released within the first 2 years of the experiment and concentrations are now close to detection limits. All cement and saltstone lysimeter sources contained higher

[1] Evaluation of multiple $NpO_2(s)$ sources indicates some variability in the total ^{237}Np content in each source despite a similar level reported by Roberts et al., (2012). The variability is likely due to the difficulty of weighing small aliquots of solid actinide sources within a HEPA filtered glovebox at Savannah River National Laboratory. Thus, a better approach is to compare total activity leached and aqueous concentrations of each radioisotope in the effluent waters to evaluate the potential for solubility control of the aqueous concentration.

concentrations of ^{60}Co in the effluent relative to a control (filter paper only containing the radioisotopes) with the gamma suite of radionuclides added directly to a filter. However, the control lysimeter contained approximately 20x lower total activity of each radioisotope. Thus, given the potential uncertainty in the source term concentrations (see footnote 1 on page 9), it is possible that similar fractions of ^{60}Co are being transported in the control, cement, and saltstone source lysimeters.

- There is a high degree of variability in the amount of water flowing through each lysimeter. It is hypothesized this is due to heterogeneous flow of water through the soil and variations in the localized climate (i.e. wind and rain patterns) above the 4" diameter lysimeter opening. Tracer experiments described below have demonstrated that preferential flowpaths exist in the lysimeters.

1. INTRODUCTION

This document describes the analysis of the effluent from lysimeters from the Radiological Field Lysimeter Experiment (RadFLEx) facility discussed in the report "SRNL Radionuclide Field Lysimeter Experiment: Baseline Construction and Implementation" by Roberts et al., (2012, SRNL-STI-2012-00603). Savannah River National Laboratory (SRNL) presently has multiple active radionuclide transport experiments under field conditions underway at the Radionuclide Field Lysimeter Experiment. A list of all lysimeters along with source radionuclides and activities is provided in Table 1.1. The timeline for deployment, capping, and removal of all lysimeters is also included in Table 1.2. In this experiment, radionuclides are buried in 5-L containers that are open to precipitation. Leachate is collected from these lysimeters approximately every three months to provide a measure of radionuclide transport through the 24" long columns. One set of 10 lysimeters contain cementitious sources. Several lysimeters were previously removed from service and sampled to determine the solid phase concentrations of radionuclides as a function of depth and also characterize the source to monitor changes which occurred during exposure to natural conditions. These solid phase analyses have been complete for some lysimeters but those studies are outside the scope of this report.

At the start of fiscal year (FY)17, there were 35 active lysimeters and 6 were removed for solid phase sampling in November 2015 leaving 29 lysimeters for subsequent sampling events. The lysimeters contain either a cementitious waste form as a source or a "soil" source. The soil sources are made by placing the radionuclide source between two

filter papers and placing the filter paper in direct contact with the soil mid-way up the lysimeter. The cementitious waste form sources are 1.25" diameter cementitous "pucks" containing the radionuclides of interest which are also placed midway up the lysimeter. The active lysimeters are:

Cementitious waste form lysimeters

- Radionuclide-free cementitious material controls (lysimeters 3 and 15)
- A suite of gamma emitters, Cs-137, Co-60, Ba-133, and Eu-152 (lysimeters 5-6 and 16-18). Note lysimeters 5 and 16 were removed on 9/15/2016 for non-destructive testing and redeployed on 04/20/2017.

Soil source lysimeters

- $Pu(V)NH_4(CO_3)$ (lysimeters 22, 23, and 42,43).
- A suite of beta/gamma emitters, Cs-137, Co-60, Ba-133, and Eu-152 (lysimeters 26-28). Note lysimeter 26 was removed on 9/15/2016 for non-destructive testing and redeployed on 04/20/2017.
- $Np(V)O_2NO_3$ and $Np(IV)O_2$ (lysimeters 30 and 32)
- $Pu(III)_2(C_2O_4)_3$ and $Pu(IV)(C_2O_4)_2$ (lysimeters 9, 10, 11, 34, 35, 39, and 40)
- $Pu(IV)O_2$ colloids (lysimeters 45 and 46)
- Sediment controls with no radionuclides (lysimeters 12, 24, 25, and 37).

Lysimeters removed from RadFLEx for soil analysis in previous years or this year are:

Cementitious waste form lysimeters

- Lysimeter 4 containing cement waste form and gamma emitters Cs-137, Co-60, Ba-133, and Eu-152, removed November 2015 for non-destructive measurements at Clemson. Lysimeter was then cut open and shipped back to SRNL for soil analysis in March 2017.

Soil source lysimeters

- $Pu(V)NH_4(CO_3)$ lysimeters 21 and 41 removed in October 2014
- $Np(V)O_2NO_3$ and $Np(IV)O_2$ lysimeters 29 and 31, respectively, removed November 2015
- $Pu(III)_2(C_2O_4)_3$ and $Pu(IV)(C_2O_4)_2$ 33 and 38, respectively, removed November 2015
- $Pu(IV)O_2$ colloids lysimeter 44, removed November 2015.

Two lysimeters (24 and 37) were constructed to be used as instrumental controls. These lysimeters were prepared identically to the other lysimeters except no source was added. These instrumented control lysimeters were fitted with two Decagon 5TM probes,

which measure soil moisture and temperature, located 20 cm and 51 cm from the top of the lysimeters. Additionally, each lysimeter was fitted with one Decagon 5TE probe, which measures soil moisture, temperature and electrical conductivity, located 36 cm from the top of the lysimeters. All of the probes collect data every 30 minutes. The data is collected during sampling of the lysimeter effluent. Another Decagon 5TE probe was placed in the soil at the site to monitor actual conditions in the field (Roberts et al., 2012).

Table 1.1: Number designations and the radioactive source descriptions and associated activities for each of the initial lysimeters in the experiment. OM = organic matter, amended in the soil of lysimeters 21, 22, and 23

Lys. No.	Lys. Description	kBq	Lys. No.	Lys. Description	kBq
1	EMPTY	-	25	Sediment Control	N/A
2	Cement Control, 4 yr*	N/A	26	Gamma suite, 2 yr	292 ^{137}Cs; 318 ^{60}Co; 248 ^{133}Ba; 470 ^{152}Eu
3	Cement Control, 10 yr	N/A	27	Gamma suite, 4 yr	
4	Cement Gamma suite, 2 yr*	4662 ^{137}Cs; 5106 ^{60}Co; 3959 ^{133}Ba; 9398 ^{152}Eu	28	Gamma suite, 10 yr	
5	Cement Gamma suite, 4 yr		29	$Np(V)O_2NO_3$, 1 yr*	45.88 ^{237}Np
6	Cement Gamma suite, 10 yr		30	$Np(V)O_2NO_3$, 4 yr	
7	Cement Tc&I, 4 yr*	9657 ^{99}Tc; 0.07 mM ^{127}I	31	$Np(IV)O_2$, 1 yr*	45.88 ^{237}Np
8	Cement Tc&I, 10 yr*		32	$Np(IV)O_2$, 4 yr	
9	$Pu(IV)(C_2O_4)_2$, Grass, 2 yr	1981 ^{239}Pu; 506 ^{240}Pu; 17585 ^{241}Pu	33	$Pu(III)_2(C_2O_4)_3$, 2 yr*	2248 ^{239}Pu; 574 ^{240}Pu; 19950 ^{241}Pu
10	$Pu(IV)(C_2O_4)_2$, Grass, 4 yr		34	$Pu(III)_2(C_2O_4)_3$, 4 yr	
11	$Pu(IV)(C_2O_4)_2$, Grass, 10 yr		35	$Pu(III)_2(C_2O_4)_3$, 10 yr	
12	Grass Control	N/A	36	EMPTY*	N/A
13	EMPTY	N/A	37	Instrumented Control	N/A
14	Saltstone Control, 4 yr*	N/A	38	$Pu(IV)(C_2O_4)_2$, 2 yr*	1981 ^{239}Pu; 506 ^{240}Pu; 17585 ^{241}Pu
15	Saltstone Control, 10 yr	N/A	39	$Pu(IV)(C_2O_4)_2$, 4 yr	
16	Saltstone Gamma suite, 2 yr	4662 ^{137}Cs; 5106 ^{60}Co; 3959 ^{133}Ba; 9398 ^{152}Eu	40	$Pu(IV)(C_2O_4)_2$, 10 yr	
17	Saltstone Gamma suite, 4 yr		41	$Pu(V)NH_4(CO_3)$, 2 yr*	2978 ^{239}Pu; 760 ^{240}Pu; 26427 ^{241}Pu
18	Saltstone Gamma suite, 10 yr		42	$Pu(V)NH_4(CO_3)$, 4 yr	
19	Saltstone Tc&I, 4 yr*	9657 ^{99}Tc; 0.07 mM ^{127}I	43	$Pu(V)NH_4(CO_3)$, 10 yr	
20	Saltstone Tc&I, 10 yr*		44	$Pu(IV)O_2$ colloids, 2 yr*	3824 ^{239}Pu; 976 ^{240}Pu; 33936 ^{241}Pu
21	$Pu(V)NH_4(CO_3)$/OM, 2 yr*	2978 ^{239}Pu; 760 ^{240}Pu; 26427 ^{241}Pu	45	$Pu(IV)O_2$ colloids, 4 yr	
22	$Pu(V)NH_4(CO_3)$/OM, 4 yr		46	$Pu(IV)O_2$ colloids, 10 yr	
23	$Pu(V)NH_4(CO_3)$/OM, 10 yr		47	EMPTY	N/A
24	Instrumented Control	N/A	48	EMPTY	N/A

N/A: Not applicable. Lysimeter does not contain radionuclides

*Lysimeters are capped in place or have been removed for solid phase analysis

Table 1.2: Dates of lysimeter deployment, capping, and removal. [a]Lysimeters are filled half-way with soil and are ready for source emplacement as needed; [b]Lysimeter 4 was opened and shipped back to SRNL for soil analysis, [c]Lysimeter removed on 9/15/2016 and a non-destructive 1-D gamma scan performed at Clemson University and lysimeter were re-deployed at RadFLEx on 4/20/2017. [d]Date of 11/2/13 has a discrepancy that is being verified with SRNL staff.

Lysimeter	Description	Source emplaced	Uncapped - start of infiltration	Capped	Capped	Uncapped	Removed[d]	Capped	Removed
1	EMPTY	a			6/13/2013	8/8/2013			
2	Cement Control, 4 yr	5/11/2012	7/5/2012		6/13/2013	8/8/2013	11/2/2013		
3	Cement Control, 10 yr	5/11/2012	7/5/2012		6/13/2013	8/8/2013			
4	Cement Gamma suite, 2 yr[b]	5/11/2012	7/5/2012		6/13/2013	8/8/2013		10/8/2015	11/5/2015[b]
5	Cement Gamma suite, 4 yr[c]	5/11/2012	7/5/2012		6/13/2013	8/8/2013		9/14/2016	9/15/2016[c]
6	Cement Gamma suite, 10 yr	5/11/2012	7/5/2012		6/13/2013	8/8/2013			
7	Cement Tc&I, 4 yr	5/11/2012	7/5/2012	3/11/2013					
8	Cement Tc&I, 10 yr	5/11/2012	7/5/2012	3/11/2013			11/2/2013		
9	$Pu(IV)(C_2O_4)_2$, Grass, 2 yr	6/20/2012	7/5/2012		6/13/2013	8/8/2013			
10	$Pu(IV)(C_2O_4)_2$, Grass, 4 yr	6/20/2012	7/5/2012		6/13/2013	8/8/2013			
11	$Pu(IV)(C_2O_4)_2$, Grass, 10 yr	6/20/2012	7/5/2012		6/13/2013	8/8/2013			
12	Grass Control	6/20/2012	7/5/2012		6/13/2013	8/8/2013			
13	EMPTY	a			6/13/2013	8/8/2013			
14	Saltstone Control, 4 yr	4/27/2012	7/5/2012		6/13/2013	8/8/2013	11/2/2013		
15	Saltstone Control, 10 yr	4/27/2012	7/5/2012		6/13/2013	8/8/2013			
16	Saltstone Gamma suite, 2 yr[c]	4/27/2012	7/5/2012		6/13/2013	8/8/2013		9/14/2016	9/15/2016[c]
17	Saltstone Gamma suite, 4 yr	4/27/2012	7/5/2012		6/13/2013	8/8/2013			
18	Saltstone Gamma suite, 10 yr	4/27/2012	7/5/2012		6/13/2013	8/8/2013			
19	Saltstone Tc&I, 4 yr	4/27/2012	7/5/2012	3/11/2013					
20	Saltstone Tc&I, 10 yr	4/27/2012	7/5/2012	1/15/2013			11/2/2013		

Table 1.2 continued.

Lysimeter	Description	Source emplaced	Uncapped - start of infiltration	Capped	Capped	Uncapped	Removed[d]	Capped	Removed
21	$Pu(V)NH_4(CO_3)$/OM, 2 yr	6/20/2012	7/5/2012		6/13/2013	8/8/2013	10/16/2014		
22	$Pu(V)NH_4(CO_3)$/OM, 4 yr	6/20/2012	7/5/2012		6/13/2013	8/8/2013			
23	$Pu(V)NH_4(CO_3)$/OM, 10 yr	6/20/2012	7/5/2012		6/13/2013	8/8/2013			
24	Instrumented Control	4/27/2012	7/5/2012		6/13/2013	8/8/2013			
25	Sediment Control	4/27/2012	7/5/2012		6/13/2013	8/8/2013			
26	Gamma suite, 2 yr[c]	4/27/2012	7/5/2012		6/13/2013	8/8/2013		9/14/2016	9/15/2016[c]
27	Gamma suite, 4 yr	4/27/2012	7/5/2012		6/13/2013	8/8/2013			
28	Gamma suite, 10 yr	4/27/2012	7/5/2012		6/13/2013	8/8/2013			
29	$Np(V)O_2NO_3$, 1 yr	5/11/2012	7/5/2012		6/13/2013	8/8/2013		10/8/2015	11/5/2015
30	$Np(V)O_2NO_3$, 4 yr	5/11/2012	7/5/2012		6/13/2013	8/8/2013			
31	$Np(IV)O_2$, 4 yr	5/11/2012	7/5/2012		6/13/2013	8/8/2013		10/8/2015	11/5/2015
32	$Np(IV)O_2$, 10 yr	5/11/2012	7/5/2012		6/13/2013	8/8/2013			
33	$Pu(III)_2(C_2O_4)_3$, 2 yr	6/20/2012	7/5/2012		6/13/2013	8/8/2013		10/8/2015	11/5/2015
34	$Pu(III)_2(C_2O_4)_3$, 4 yr	6/20/2012	7/5/2012		6/13/2013	8/8/2013			
35	$Pu(III)_2(C_2O_4)_3$, 10 yr	6/20/2012	7/5/2012		6/13/2013	8/8/2013			
36	EMPTY	a							
37	Instrumented Control	4/27/2012	7/5/2012		6/13/2013	8/8/2013			
38	$Pu(IV)(C_2O_4)_2$, 2 yr	6/20/2012	7/5/2012		6/13/2013	8/8/2013		10/8/2015	11/5/2015
39	$Pu(IV)(C_2O_4)_2$, 4 yr	6/20/2012	7/5/2012		6/13/2013	8/8/2013			
40	$Pu(IV)(C_2O_4)_2$, 10 yr	6/20/2012	7/5/2012		6/13/2013	8/8/2013			
41	$Pu(V)NH_4(CO_3)$, 2 yr	6/20/2012	7/5/2012		6/13/2013	8/8/2013	10/16/2014		

Table 1.2 continued.

Lysimeter	Description	Source emplaced	Uncapped - start of infiltration	Capped	Capped	Uncapped	Removed[d]	Capped	Removed
42	$Pu(V)NH_4(CO_3)$, 4 yr	6/20/2012	7/5/2012		5/14/2013	8/8/2013			
43	$Pu(V)NH_4(CO_3)$, 10 yr	6/20/2012	7/5/2012		5/14/2013	8/8/2013			
44	$Pu(IV)O_2$ colloids, 2 yr	5/11/2012	7/5/2012		5/14/2013	8/8/2013		10/8/2015	11/5/2015
45	$Pu(IV)O_2$ colloids, 4 yr	5/11/2012	7/5/2012		5/14/2013	8/8/2013			
46	$Pu(IV)O_2$ colloids, 10 yr	5/11/2012	7/5/2012		5/14/2013	8/8/2013			
47	EMPTY				5/14/2013	8/8/2013			
48	EMPTY				5/14/2013	8/8/2013			

2. DATA REPORTING and TIMEKEEPING

In previous reports the data were described based on the fiscal year (FY) and quarter (Q) in which samples were collected. This was a convenient method at the time but inherently causes problems when sampling events are missed or there are multiple sampling events in one quarter. Therefore, in this report the current sampling events are described using the date of sampling. For example, samples collected on July 14, 2015 are labeled 150714. This is the sampling ID protocol being used by Savannah River National Laboratory (SRNL) collaborators when collecting the field samples. Therefore, to maintain consistent records, a list of sampling dates, SRNL sample IDs, and the ID used in this report to note the entire sampling event are provided in Table 2.1. The electronic database accompanying this report uses this same ID format (described below).

Table 2.1: List of Sample dates and IDs from RadFLEx effluent sampling.

Sampling Date(s)	SRNL Sample ID range (notation is year-month-date of sample collection)	ID used in this report to describe sampling event (ID used in previous reports)
10/4/2012	121004	100412 (FY13Q1)
1/9/2013	130109	130109 (FY13Q2)
3/2/2013-3/7/2013	130212-130307	130212-130307 (FY13Q3)
5/14/2013-6/13/2013	130514-130617	130514-130617 (FY13Q4)
11/5/2013-11/6/2013	131105-131106	131105-131106 (FY14Q1)
2/10/2014	140210	140210 (FY14Q2)
5/5/2014	140505	140505 (FY14Q3)
7/16/2014	140716	140716 (FY14Q4)
11/5/2014	141105	141105
1/6/2015	150106	150106
3/26/2015	150326	150326
7/14/2015	150714	150714
10/8/2015	151008	151008
12/16/2015	151216	151216
3/1/2016	160301	160301
6/1/2016	160601	160601
08/09/2016	160809	160809
02/07/2017	170207	170207

3. BACKGROUND

Project overview

Understanding the geochemical behavior and vadose zone transport of radionuclides produced during nuclear weapons development and generated during nuclear power production is very important when determining a long-term storage solution for radioactive waste. Long-lived actinides, such as neptunium and plutonium (predominantly ^{237}Np and ^{239}Pu), as well as the fission and activation products ^{137}Cs and ^{99}Tc are risk driving radionuclides under release or disposal scenarios due to either their half-life, environmental mobility, or quantity produced. Subsurface transport of these elements is influenced by many factors including sorption, oxidation and reduction, complexation, and precipitation reactions (Choppin, 2006; Cleveland, 1979; Kaplan et al., 2006a and 2006b; Kaszuba and Runde, 1999; Kim et al., 2006; Madejon, 2012). A greater understanding of this behavior will help to develop more robust geochemical models and reduce conservatism in performance assessments (PAs). Laboratory experiments provide valuable data but there is a need to supplement this data with field scale experiments that can be performed under more representative environmental conditions. For example, several studies have examined the transport of plutonium using field lysimeters and used lab scale data to conceptualize the field scale reactive transport models (Kaplan et al., 2004; Kaplan et al., 2006a and 2006b).

Lysimeters are field columns packed with sediment and containing a source amended with a radionuclide of interest placed at the midpoint of the soil column. The lysimeters are left exposed to rainfall and field conditions. The effluent is collected and

analyzed for the contaminant initially amended in the source. Following a defined timescale for effluent collection, the lysimeters are cored and the concentrations of the contaminant in the solid phase are determined.

Early studies by Kaplan et al., (2004, 2006a, 2006b) provided valuable information about plutonium behavior in the vadose zone. The lysimeters contained sources of a known activity and oxidation state of plutonium and were left exposed to environmental conditions for approximately 2 and 11 years. The majority (>95%) of the plutonium remained within 2 cm of the source and in the Pu(IV) oxidation state. This is expected based on the higher mobility of Pu(VI) relative to Pu(IV). Another important discovery from these works was the observed upward migration of plutonium. Demirkanli et al., (2008, 2009) and Thompson et al., (2012) provided strong evidence that this upward migration was caused by uptake in grass roots that grew naturally on the surface of the lysimeters during the experiment. More accurate simulations were developed by including partitioning coefficients between plutonium and the grass roots (Demirkanli et al., 2009). Laboratory studies of plutonium uptake and mobility in corn were also performed and provided additional support for this explanation (Thompson et al., 2012).

Lysimeter soil and source description

The RadFLEx facility was designed to address the knowledge gaps from the previous work with Pu bearing lysimeters mentioned above (Roberts et al., 2012). RadFLEx initially deployed 43 lysimeters with controls or radionuclide bearing sources. Several lysimeters were removed for solid phase analysis and there are currently 29

active lysimeters as described in Tables 1.1 and 1.2. Leachate is collected from these lysimeters every three months to provide a measure of radionuclide transport through the columns. Lysimeters containing plutonium sources were installed in triplicate so that soil profile analysis can be performed at three discrete time intervals. Analysis was only performed after 2 and 11 years during the original study Kaplan et al. (2004, 2006a). One set of lysimeters contains plutonium sources amended with NOM. The sorption capacity and solubility of Pu(IV) is strongly influenced by NOM due to the formation of Pu-NOM complexes (Santschi et al., 2002; Zimmerman et al., 2014). Additionally, one set of lysimeters containing plutonium sources contains vegetation in order to verify the effect of plant roots on the upward migration of plutonium. There are also two sets of lysimeters containing Np(IV) and Np(V) sources that can be used as oxidation state chemical analogs of plutonium.

This study will also provide data that are relevant to performance assessment models at SRS examining reducing grout based waste forms. SRS currently contains approximately 100 million liters of radioactive waste in 51 underground storage tanks, 43 of which are still operational. The waste in these tanks is in two forms: an insoluble mixture of metal hydroxides and a soluble salt. The soluble salt form makes up 93% of the total waste volume. Treatment of the salt waste is performed by solidifying the waste in a solid form called saltstone. Saltstone is a mix of Portland cement, fly ash, and blast furnace slag, which serves as a reducing agent.

The saltstone sources in this work are composed of a 45:45:10 premixture ratio of fly ash, slag, and cement, respectively (Roberts et al., 2012). Roberts and Kaplan (2009)

used the methods described by Angus and Glasser (1985) to measure the reduction capacity of the slag component which is assumed to provide reduction capabilities of saltstone. The reported value of 819 μeq g^{-1} is consistent with values determined in similar studies (Kaplan et al. 2009; Lukens et al. 2005).

The radioactive constituents contained in the salt waste, ^{60}Co, ^{137}Cs, ^{133}Ba, and ^{152}Eu, were chosen for this work in order to examine monovalent (^{137}Cs), divalent (^{60}Co and ^{133}Ba) and trivalent (^{152}Eu) cation release from the saltstone. Lysimeters 16-18 contain saltstone sources amended with a suite of the gamma emitting ^{60}Co, ^{137}Cs, ^{133}Ba, and ^{152}Eu. Lysimeters 4-6 contain cement sources (a mixture of fly ash and cement with no slag present) amended with the suite of gamma emitters.

Soil and effluent characterization

The primary purpose of this work is to analyze samples from the RadFLEx facility, interpret the data, and provide any necessary explanation and support for the findings. The experiment began in May 2012 and is expected to span a ten-year period. This work includes measurements of quarterly effluent sampling events and analysis of any radionuclides measured in appreciable quantities during this period.

The RadFLEx facility is located at SRS in Aiken, SC. Each lysimeter (24" long and a 4" diameter) has a volume of 4,118.5 cm^3 (1.09 gallons) that is uncapped at the top end allowing exposure to environmental conditions (Roberts et al., 2012). The lysimeters are all packed with a single, homogenized soil from the SRS which is a representative end member soil found at SRS. Specific chemical and physical characteristics of the soil are shown in Table 3.1 (Roberts et al., 2012). Additional mineralogical and elemental

characterization was performed this year. These measurements are included in Table 3.2 and 3.3. The primary mineral phases are kaolinite and quartz. Unexpectedly, no goethite or hematite was observed in the x-ray diffraction (XRD) pattern. This is despite a relatively high iron content in the soil. It is hypothesized that the iron content is present as small disordered phases as coatings on quartz particles or incorporated into phyllosilicates. However, this proposed iron mineralogy remains to be proven.

Table 3.1: Characterization of soil obtained from Central Shops Borrow pit at the Savannah River Site (Roberts et al., 2012).

Analysis	Lysimeter Soil	Lysimeter Soil +OM[1]
pH	5.27	4.89
Organic-Carbon (%)	0.085	1.704
Organic-Nitrogen (%)	0.008	0.062
Organic-Sulfur (%)	0.012	0.018
Sand (%)[2]	66	Not Meas.
Silt (%)[2]	14	Not Meas.
Clay (%)[2]	20	Not Meas.
Surface Area (m^2 g^{-1})	9.14	Not Meas.
CEC[3] (meq $100g^{-1}$)	1.73	5.56
Base Saturation (%)	27.62	14.21
CDB[4] Fe (mg g^{-1})	6.01 ± 0.68	NM[5]
CDB Al (mg g^{-1})	1.978 ± 0.20	NM[5]
Total Fe (ppm)	8,101	13,180
Total Mn (ppm)	7.29	7.72
Total P (ppm)	36.6	<6
Total S (ppm)	112.2	111.5

[1]OM = organic matter, amended in the soil of lysimeters 21, 22, and 23.
[2]Measurement by Daniel B. Stephens Laboratory
[3]CEC = Cation exchange capacity
[4]CDB = Citrate-Bicarbonate-Dithionite extractable
[5]NM = Not measured

Table 3.2: Mineralogical fractions determined using powder X-ray diffraction by The Mineral Lab, Inc. (Golden, CO).

Phase	Whole Soil	<2um size fraction
Kaolinite	58	>95
Quartz	39	<2
Unknown	<5	<5

Table 3.3: Elemental X-ray Fluorescence analysis of soil composition. The balance of the percentages (approximately 10%) is due to chemically and physically sorbed water and other trace minerals.

Phase	Percentage
MgO	0.14
Al_2O_3	13.6
SiO_2	72.9
K_2O	0.09
CaO	0.08
TiO_2	0.47
Fe_2O_3	2.64
BaO, MnO_2, Cl, S, P_2O_5, Na_2O	< 0.05%

Overview of Radionuclide Geochemical Behavior

Cobalt

Cobalt-60 (^{60}Co), a fission product, was chosen for this study in order to examine transport of divalent cations. In terrestrial environments, aqueous ^{60}Co is found in the Co(II) and Co(III) oxidation states with Co(II) being the dominant state (Collins and Kinsela, 2010). Cobalt mobility in soil is dependent on pH with approximately an order of magnitude variation in K_d values for a unit of pH change in the soil. Due to its low solubility, Co(III) will only be present in aqueous solutions if complexed with a strong

chelating agent (Duckworth et al., 2009). Studies of ^{60}Co speciation in groundwater as a result of contamination from nuclear waste repositories have shown that when deposited with a strong chelating agent (i.e., ethylenediaminetetraacetic acid [EDTA]) anionic EDTA complexes dominate ^{60}Co speciation (Caron and Mankarios, 2004; Robertson et al., 1995). The oxidation of the Co(II)-EDTA complexes is most likely due to solid phase Fe(III) oxyhydroxides and Mn(IV) oxides (Collins and Kinsela, 2010).

Plutonium

Plutonium (Pu) mobility in soil is largely governed by its oxidation state. Plutonium is unique in that it may simultaneously exist as reduced Pu(III/IV) and oxidized Pu(V/VI) in a given system (Cleveland, 1979). Geochemical behavior, such as complexation strength and hydrolysis of Pu increases with increasing effective charge of the ion (Choppin, 1983):

$$\underset{+4.0}{Pu(IV)^{4+}} > \underset{+3.2}{Pu(VI)O_2^{2+}} > \underset{+3.0}{Pu(III)^{3+}} > \underset{+2.2}{Pu(V)O_2^{+}}$$

The increased effective charge of the plutonyl (i.e. Pu(V) and Pu(VI)) oxidation states is due to the axial oxygen atoms (Kim, 1986). Far field transport of Pu has also been facilitated by the presence of colloids with kilometer scale transport observed at the Nevada Test Site (Kersting et al., 1999). Previous lysimeter experiments of Pu transport in SRS soils have shown the importance of the oxidation state of the source and oxidation and reduction reactions on Pu mobility (Kaplan et al., 2004, 2006a, 2006b). An 11-year field lysimeter study analyzed by Kaplan et al. (2004) employed four lysimeters containing three reduced sources (one Pu(III) and two Pu(IV)) and one oxidized source

(Pu(VI)). The main finding was that in each lysimeter, 95% of the Pu was found within 1.25 cm from the source. Reactive transport modeling and oxidation state analysis of the Pu within the soil showed that >90% was as the immobile Pu(IV) (Kaplan et al., 2004; Kaplan et al., 2006a). Decreasing concentrations of Pu with depth were found in the reduced Pu lysimeters as far as 40 cm from the surface. It is evident that in these lysimeters Pu underwent cyclic oxidation and reduction. This conceptual model is consistent with the wetting and drying cycles within the lysimeter soil profile where penetrating water will cause Pu oxidation and subsequent downward movement. Drying will then cause Pu reduction to the immobile Pu(IV) state.

The RadFLEx facility includes 18 lysimeters that contain Pu sources in the +3, +4, and +5 oxidation states. Lysimeters 9, 10, and 11 have been amended with grass in order to observe the effect of vegetation and lysimeters 21, 22, and 23 were amended with organic matter in order to observe the potential of organic matter to enhance the mobility of Pu (Roberts et al., 2012). Lysimeters 33-35 and 38-46 contain Pu sources with no additional amendments. The addition of vegetation was made because the upward migration of Pu observed in the previous lysimeter studies has been attributed to plant root uptake (Demirkanli et al., 2009, Kaplan et al., 2010, Molz et al., 2014). Experimental data and modeling agreement suggest that the grass allowed to grow on the lysimeters was responsible for transport up in the root xylem and into the above-ground parts of the plant. This would result in Pu deposition on the surface of the lysimeter during die-back with any remaining Pu in the roots diffusing back into the soil. The rate of uptake in the grass roots is 5×10^6 times faster than in corn (Molz et al., 2014) and

likely contributed to the majority of the Pu concentration measured above the source. Another possible contribution to the upward migration is a vertical soil water flow to roots that is not a parameter in current 1-D modeling approaches, such as microbial chemotaxis (Molz et al., 2014). The set of lysimeters with well characterized sources that have been amended with Bahia grass will be very useful in validating previous concepts and conjectures. The breadth of the sources and amendments of the Pu lysimeters will increase the understanding of Pu mobility through sediment gained from the previous studies, though the results from those studies suggest that little to no Pu breakthrough will occur for the planned 10 year duration of the RadFLEx experiments.

Neptunium

Due to its long half-life (2.14×10^6 years) and its relatively fast mobility in the subsurface, the contribution of neptunium (Np) to the radiation inventory in nuclear waste repositories is an important consideration. The Np(IV) and Np(V) oxidation states may exist in the environment. However, in mildly oxic aqueous conditions, Np(V) is the dominant species (Kaszuba and Runde, 1999). The high solubility of the solid phases and weak sorption of Np(V) make it very mobile under most environmental conditions. Tetravalent neptunium is more commonly found under highly reducing conditions and is far less mobile due to its lower solubility and greater tendency to form surface complexes (Kaszuba and Runde, 1999).

Previous work has been performed that studied sorption of Np(V) to SRS soil (Miller, 2010). Desorption experiments showed that sorption was completely reversible, thus allowing for simulation using either K_d values or standard surface complexation

models. Additional sorption experiments in the presence of NOM and other reducing agents, that would promote competition for sorption, had little effect on sorption behavior. The sorption data was modeled using a diffuse-double layer model and calibrated using citrate-bicarbonate-dithionite (CDB) extractable iron content. It was determined that 4% of the soil Fe was reactive with Np. The sorption data were modeled using 1:1 (pH values less than 7) and both 1:1 and 2:1 (pH values greater than 7) Np: FeOH surface complexes which reacted with the 4% of reactive iron content in the soil (Miller, 2010). These findings can be exploited for modeling Np transport in the RadFLEx study because only the aforementioned surface complexes need to be considered.

4. MATERIALS AND METHODS

Lysimeter Design

The construction of the lysimeters used in this experiment is described in Roberts et al., 2012. The lysimeters are made from 24" length by 4" diameter polyvinyl chloride (PVC) pipes. A 4" to 2" reducer is placed at the bottom of the pipe to hold a perforated polypropylene grid supporting a nylon mesh screen (80 x 80 mesh, McMaster Car part # 9318T17) meant to prevent sediment from passing through into the effluent collection bottles. The 4" to 2" reducer is connected to a 2" bushing which is fitted with a ¾" barbed nipple. Nylon Tygon tubing is attached to the nipple to guide the effluent water into the collection bottles. Based on calculations using the average volume of water passing through the lysimeters, there should be no restriction of flow through this configuration. The lysimeters are housed in a 6" diameter PVC pipe with a 6" to 4" reducing bushing for the purpose of secondary containment. A small section of 4" PVC is glued into the bushing and coupled to another 4" to 2" reducer with a 2" PVC pipe that collects effluent for the secondary containment. The secondary containment serves not only as double containment consistent with radiological protection but also as a collection mechanism should any overflow occur from the lysimeters. A secondary but very important benefit of this design is that extraction of the lysimeters can be accomplished with relative ease. Images of the lysimeter components and schematic are shown in Figures 4.1 and 4.2, respectively.

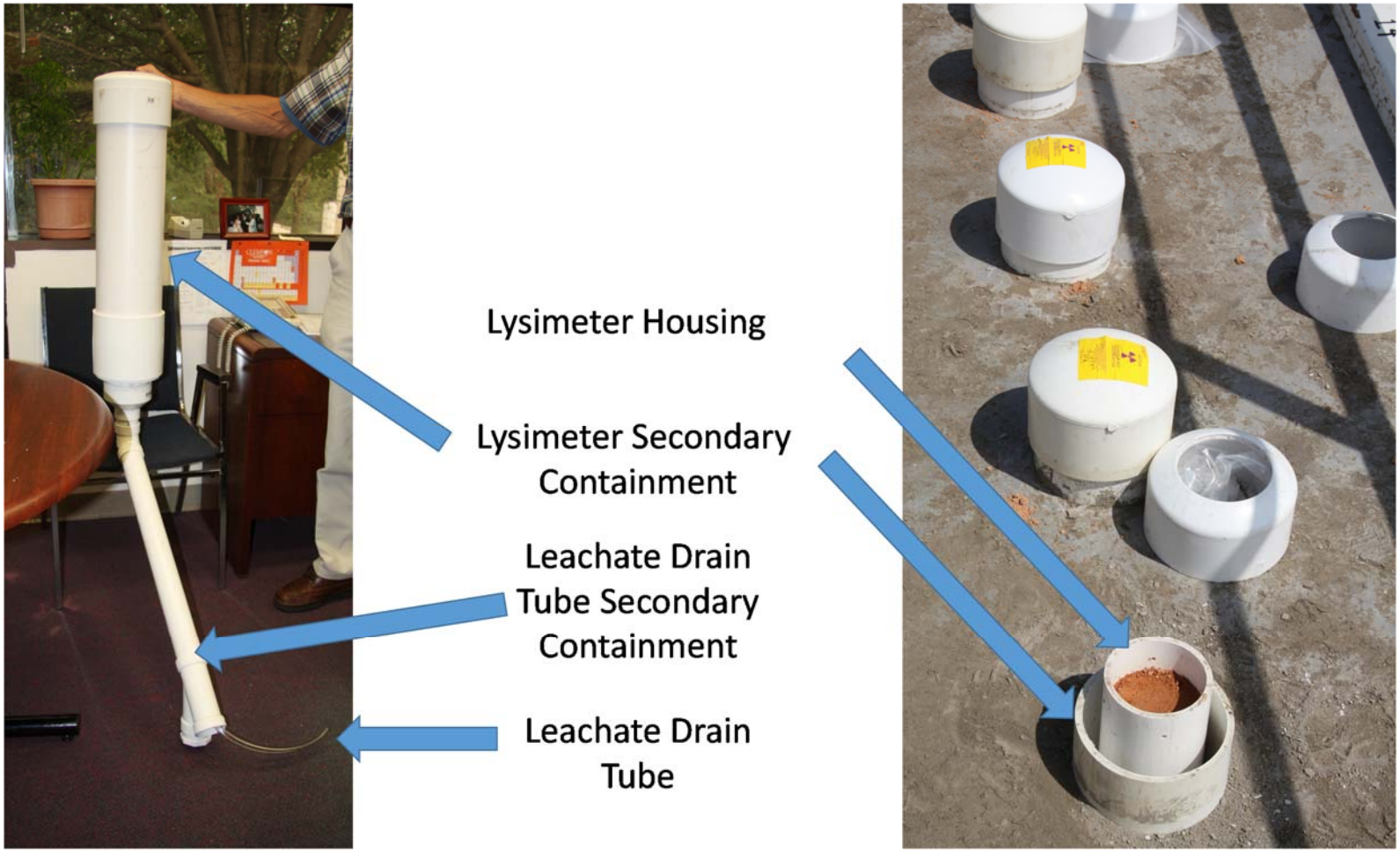

Figure 4.1: Design components of the lysimeters (Roberts et al., 2012).

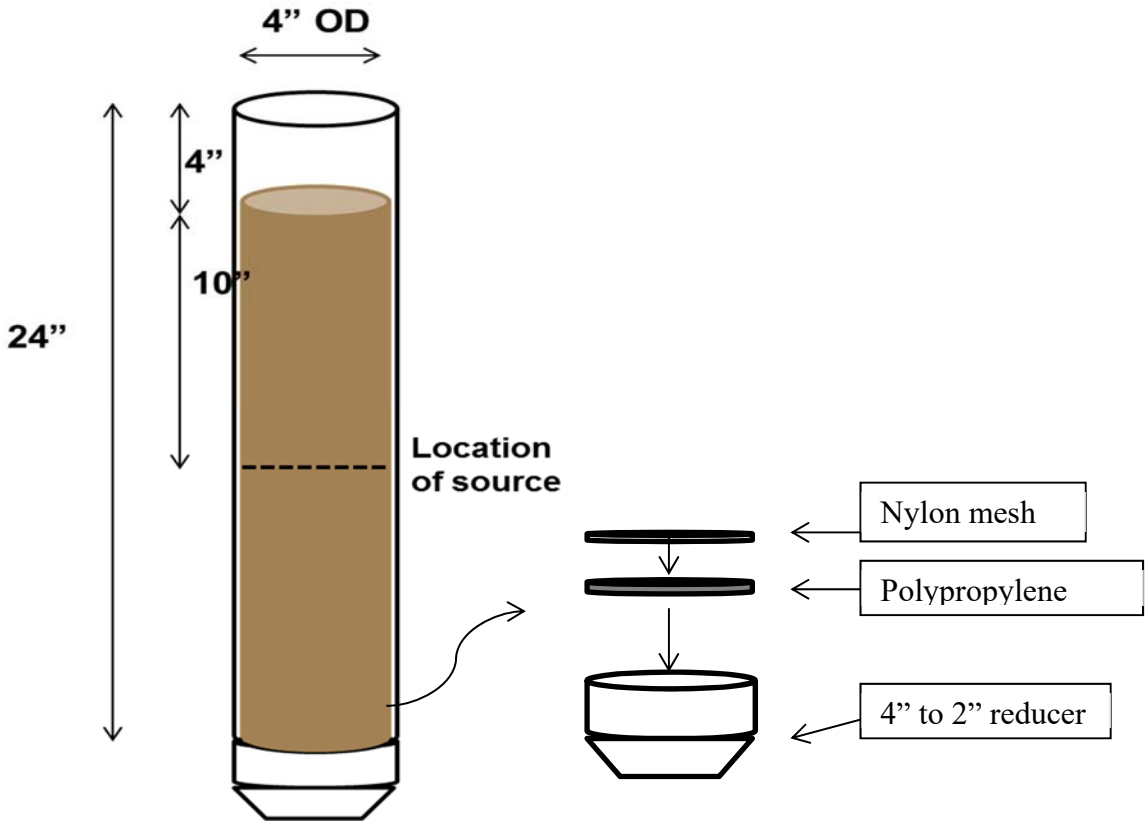

Figure 4.2: Schematic of the lysimeters. The nylon mesh was glued to the bottom of the PVC pipe. Then the polypropylene grid was glued on the bottom of the PVC pipe. Finally, 4” to 2” reducer was fitted over the bottom of the pipe. The purpose of the reducer was also to keep the nylon mesh and grid in place.

Data Recording

All measurements and observations were recorded in a laboratory notebook with the appropriate title, time, date, and apparatus used. A sample datalog sheet, that includes the unique sample and subsample code identification (ID), dates of sample collection, receipt from SRS and dates of sample preparation and analysis at Clemson,

was created for each received sample. Preliminary measurements and subsampling information were also recorded on these datalog sheets. An example datalog sheet can be found in Appendix A.

The high purity germanium detectors (Model: GC2519, SN: 08017390 and Model: GC4018, SN: 1933074) and Thermo Scientific inductively coupled plasma mass spectrometer (ICP-MS) (Model: X-2, SN: 012990) were calibrated with National Institute of Standards and Technology (NIST) traceable standards. The calibration date, standard identification and expiration dates, and quality assurance and quality control (QA/QC) spiked samples were recorded on a calibration datasheet for each sampling event. An example datasheet for calibration can be found in Appendix A.

Sample Receipt and Subsampling

Lysimeter effluent samples have been received in 2 L bottles on a quarterly basis since October 2012. Effluent samples are collected and shipped by SRNL collaborators Dr. Dan Kaplan and Dr. Kimberly Roberts. The methods described below have been used for the samples that have been received to this point and will be used for future samples. Approximately 250 mL, (or half of the total volume if the sample volume was less than 500 mL) of each lysimeter effluent sample was removed for archiving and placed into a 250 mL high-density polyethylene (HDPE) pre-cleaned container. The ID given to each subsample was also used for the archived containers. The pH and dissolved oxygen (DO) content of each received solution was measured using a Thermo Ross semi-micro pH electrode and a VWR (VWR, Inc.) DO probe. The pH electrode was standardized with

Thermo pH buffer solutions at pH values of 4.01, 7.00 and 10.04. Archive information and pH and DO measurements were recorded on subsample datalog sheets.

Lysimeter effluent bottles were acidified to 2% nitric acid (HNO_3) using concentrated nitric acid. The intent of acidifying the solutions within the leachate collection bottles was to facilitate desorption of any ions sorbed to the container walls. Thus the 250 mL archived subsample removed is to preserve the sample in the "field" (non-acidified) state in the event that analysis of radionuclide speciation is to be performed at a future date. Samples for analyte measurements were taken from the acidified sample. In the event that there was a measurable quantity of a radionuclide in the acidified subsample, then inferences based on conceptual knowledge radionuclide speciation could be made. For example, if measureable quantities of plutonium were made in the acidified subsample from a lysimeter containing a Pu source, then it could be assumed that the Pu in the un-acidified bottle was in the +4 oxidation state, due to the high sorption affinity of Pu in this oxidation state. If measurement of the un-acidified sample did not indicate the presence of Pu, then the concentration could then be determined in the original, un-acidified subsample by using dilution calculations. Additionally, oxidation state analysis of the acidified sample could verify these inferences. Any samples and subsamples taken from the acidified bottles were referred to as the sample ID with the suffix –Acid in subsample containers and data files.

Minimum Detectable Concentrations

The lower limits of detection (LLD) were determined for each radionuclide. The LLDs were then used to calculate the minimum detectable concentrations (MDCs) using

the Currie Equation (Equation 1). The MDC calculated for radionuclides in this work, for each sampling event, are reported in Table 4.1

$$MDC = \frac{LLD}{\epsilon \times t \times f \times V} \qquad \text{(Currie, 1968) (1)}$$

LLD = Lower limit of detection (counts)
ϵ = efficiency (-)
t = count time (s)
f = Branching ratio (-)
V = Volume of subsample (L)

Table 4.1: Minimum detectable concentration calculated for effluent analysis. ND: Not determined.

Sampling Event	^{60}Co[1]	^{137}Cs[1]	^{133}Ba[1]	^{152}Eu[1]	^{237}Np[2]	$^{239/240}$Pu[2]
121004	4.98E+01	3.77E+00	2.92E+00	4.66E+01	ND	ND
130109	3.81E+00	5.17E+00	1.12E+01	1.42E+02	ND	ND
130212-130307	3.97E+00	4.26E+00	1.21E+01	1.52E+02	1.49E-01	9.86E-02
130514-130617	3.97E+00	4.99E+00	1.21E+01	1.52E+02	8.34E-04	2.45E-01
131105-131106	6.10E+00	5.80E+00	9.43E+00	1.33E+02	2.60E-04	1.38E-01
140210	4.52E+00	5.66E+00	1.09E+01	1.58E+02	1.48E-03	1.72E-01
140505	5.39E+00	7.31E+00	1.39E+01	1.71E+02	4.69E-04	1.58E-01
140716	4.22E-02	7.08E-02	1.26E-01	1.66E+00	2.45E-03	2.39E-01
141105	1.27E+00	1.35E+00	2.56E+00	3.14E+01	4.17E-04	9.18E-02
150106	2.28E+00	2.58E+00	5.47E+00	7.73E+01	1.00E-04	6.58E-01
150326	2.28E+00	2.58E+00	5.47E+00	7.73E+01	1.00E-04	6.58E-01
150714	1.42E+00	3.94E+00	5.00E+01	1.57E+02	1.26E-04	5.28E-02
151008	1.35E+00	1.44E+00	2.78E+02	3.36E+01	6.80E-05	8.70E-05
151216	1.35E+00	1.44E+00	2.78E+02	3.36E+01	6.80E-05	8.70E-05
160301	1.81E+00	6.31E+00	2.31E+02	8.06E+01	2.50E-05	8.24E-04
160601	3.43E+00	6.42E+00	1.86E+02	4.28E+02	2.50E-05	2.50E-05
160809	2.67E+00	1.99E+00	5.11E+00	6.86E+01	2.82E-04	1.48E-03
170207	4.09E+00	5.85E+00	1.00E+01	1.22E+02	1.90E-05	3.00E-06

[1] Values based on background count rate and efficiency in the region of interest of the gamma energy for the respective isotope. Values reported in Bq L^{-1}
[2] Values based on ICP-MS intercept concentration values reported in ppb (μg L^{-1}).

Analysis of Gamma Emitting Radionuclides (^{60}Co, ^{137}Cs, ^{133}Ba, ^{152}Eu)

Samples containing gamma emitting radionuclides were analyzed using a high purity germanium detector (HPGe). One HPGe (Model: GC4018, SN: 1933074) was used for analysis of the samples collected during the first several sampling intervals (121004, 130109, 130212-130307, 130514-130617, 131105-131106, 140210) sampling intervals and another HPGe (Model: GC2519, SN: 0817390) was used for analysis of the samples collected during the subsequent sampling intervals. Quarterly efficiency calibrations of the germanium detectors were performed using a NIST traceable ^{152}Eu stock solution. An example calibration curve sampling event, 121004, is shown below (Figure 4.3). As noted on the y-axis, the efficiency varied between 0.5% to 2.5% for the energy range examined. A standard geometry of 45mL of sample in a 50mL conical polypropylene centrifuge tube was used. The tube was placed in a plastic Marinelli beaker fitted to cover the detector and counted for 24 hours. A quarterly background radiation measurement was made by counting a sample tube filled with the standard amount (45 mL) of distilled deionized (DDI) water. The background count rate and the efficiency for each isotope were used to calculate the MDC. The MDC are listed in Table 4.1.

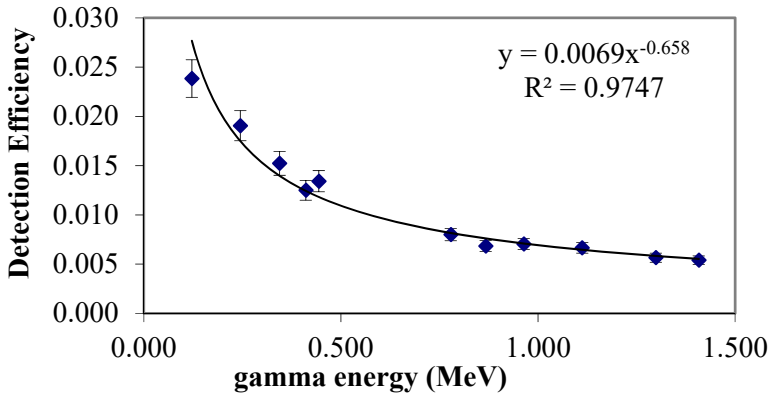

Figure 4.3: HPGe Efficiency curve determined from counting 45 mL of a ^{152}Eu standard in a 50 mL conical centrifuge tube.

Determination of Activity

The list of gamma decay energies and associated intensities used to determine the activities of ^{60}Co, ^{137}Cs, ^{133}Ba, and ^{152}Eu are shown in Table 4.2 (National Nuclear Data Center, 2014). The gamma energies in Table 4.2 were chosen because they were emitted with the highest intensities. The activity of ^{137}Cs was determined by the count rate for the 0.662 MeV decay energy. The activities of ^{60}Co, ^{133}Ba, and ^{152}Eu were calculated by taking the average of the activities based on the count rates associated with the gamma energies in Table 4.2. The error for ^{137}Cs was calculated using counting statistics assuming a 2σ confidence in the average error associated with the efficiency calibration curve, which was 8%. The error for ^{60}Co, ^{133}Ba, and ^{152}Eu was calculated using the standard deviation of the activity measurements based on the gamma decay energies.

Table 4.2: Gamma decay energies and associated intensities of the gamma emitting radionuclides that were used to calculate the activities of the respective radionuclides.

Radionuclide	Gamma Decay Energy (MeV)	Intensity (unitless)
^{137}Cs	0.662	0.851
^{60}Co	1.173	0.999
	1.332	0.999
^{133}Ba	0.081	0.329
	0.303	0.183
	0.356	0.621
^{152}Eu	0.411	0.022
	0.778	0.129
	1.089	0.017

Analysis of the actinides (^{237}Np and $^{239/240}$Pu)

Analysis of samples containing ^{237}Np and $^{239/240}$Pu was performed using a Thermo Scientific ICP-MS (Model: X-2, SN: 012990). Approximately 10 mL of acidified sample was removed from the collection bottles and placed in a 15mL centrifuge tube and subsequently analyzed on the ICP-MS. ^{237}Np and ^{239}Pu concentration standards were prepared by diluting NIST standard reference materials 4341 and 4330C for ^{237}Np and ^{239}Pu, respectively. The samples were run using ^{242}Pu as an internal standard to account for changes in flow rate and any changes in sensitivity due to external factors such as fluctuations in temperature, pressure, or humidity. The minimum detectable concentrations for ^{237}Np and ^{239}Pu are based on the intercept concentrations of the calibration curves and are shown in Table 4.1 for each of the sampling events.

Selected Major Ion Concentrations

In addition to the determination of radionuclide concentrations, the concentrations of selected major ions were determined for all sampling events and can be found in the

database accompanying this report. The concentrations were determined using ICP-MS. Calibration standards were prepared by diluting NIST traceable multiple element standards. The ions monitored in the effluents from the first three sampling events were potassium (K), magnesium (Mg), iron (Fe), zinc (Zn), and manganese (Mn). Due to the availability of calibration standards, the ions monitored in the effluents from the subsequent sampling events were sodium (Na), Mg, K, calcium (Ca), Mn, and Fe. These concentrations were determined in order to monitor the concentration of major ions to provide an estimation of the ionic strength of the solution and to determine the potential for competition between these major ions and the radionuclides of interest.

Low-level $^{239/240}$Pu measurements

The detection limit for ^{239}Pu using the standard ICP-MS based technique is approximately 1 x 10^{-12} M. To determine if Pu was indeed present in the effluent, a separate method was employed for select samples. This method was performed on at least 1l effluent samples that were spiked with 2 ml of the ^{242}Pu tracer (0.038 Bq/ml, 0.076 Bq total added) after acidification. Then, an Fe^{3+} solution ($FeCl_3$, 10 mg Fe/ml) was added such that a Fe concentration in the sample of 200 mg /l was obtained. Then, the pH was adjusted to approximately pH 7 using concentrated NH_4OH. This leads to co-precipitation of Pu along with $Fe(OH)_3$. The solution was left to settle overnight. Then, the samples were centrifuged at 4000 rpm for 30 minutes (model: Allegra X-22R, Beckman Coulter). The supernatant was discarded and the solid washed with a dilute NH_4OH solution then the solid was dried overnight.

The precipitate was dissolved in 5 ml concentrated HNO_3 and diluted with DDI water to 3M HNO_3. Then a sufficient amount of a solid $NaNO_2$ was introduced to produce a 0.025M $NaNO_2$- 3 M HNO_3 solution.

The Pu was extracted from the resulting HNO_3-$NaNO_2$ solution using TEVA extraction chromatography resin. TEVA columns were prepared by adding 1 mL of the resin in a 2 ml column (Poly-prep chromatography columns, Bio-Rad). When gravity flow was not sufficient, a vacuum extraction system was used to control the flow rate. The column was rinsed with 5 column volumes of 3M HNO_3-0.025M $NaNO_2$. Then the sample solution was loaded onto the TEVA column. After the sample was loaded, the column was rinsed with 15 ml 3M HNO_3-0.025M $NaNO_2$. To elute plutonium from TEVA Resin, 5 column volumes of 0.01 M hydrochloric acid – 0.2M HF were used.

The Pu fraction was evaporated and dissolved with concentrated HNO_3 and 30% H_2O_2 and fumed three times in order to destroy organic compounds. Afterwards, the sample was dissolved in 0.3 ml concentrated H_2SO_4 and diluted to 0.5 M by adding DDI water. Then, the pH was adjusting between 3.2-3.5 by adding a small amounts of 10 M NaOH, using a methyl yellow pH indicator to determine the optimal pH was reached. The solution was then electroplated for 2 h using currents of 0.5 mA per sample and the samples were measured about 4 days in an Alpha Spectrometer (EG&G Ortec, Octete PC). The efficiency calibration of the detectors was performed using a NIST traceable electroplated alpha emitting radionuclide standard (^{235}U, ^{238}U, ^{239}Pu, and ^{241}Am) leading to an efficiency around 0.07. The background count rate and the efficiency for each isotope were used to

calculate the MDC using equation 1. The error for $^{239,240}Pu$ was calculated using counting statistics.

Tracer studies in packed soil columns

To demonstrate the occurrence of preferential flow, a series of tracer studies were performed using ReO_4^- and NaCl tracers as well as a visible blue dye. A 4-inch diameter PVC pipe was packed with 7 inches of soil with a density of 1.23 g/cm^3 and soil moisture of 0.18. Then, five 140 mL aliquots of a NaCl-Re (10 mM NaCl and 10 ug/L ReO_{4-}) tracer were added to the column as a "pond" on the top of the soil. This was followed by two 140 mL aliquots of a blue dye tracer. Each aliquot was added in a 15-minute interval. Effluent from the lysimeter was collected by a fraction collector in 20-second intervals for analysis. Effluent was weighed to determine volume of each fraction, then conductivity was measured. The conductivity of the original tracer solution is 17.85 mS/cm. The concentration of ReO_4^- in the effluent was determined using ICP-MS. After allowing several hours for gravity drainage of the column, the soil was extruded in sections and pictures were taken to show the occurrence and distribution of the blue dye.

5. RESULTS AND DISCUSSION

Database development

A major activity of the FY16 effort described in this report was the development of a database containing all data collected to date on this project. The database was developed in Microsoft Excel to allow easy manipulation of the data and a copy of the database is provided with this report. The key aspects of the database include:

1. A page listing all relevant metadata for the lysimeters including measured pH, DO, water volume, radionuclide concentrations with associated uncertainty, and major ion concentrations with associated uncertainty.
2. A link to the raw datafiles and data processing files used to determine the values reported with the metadata.
3. A listing of the analytical or radioanalytical detection limits for each lysimeter effluent sampling event.
4. A link to the raw background and detection limit calculations.
5. A convenient color coding of the metadata cells to note issues with the sample including: 1) insufficient sample volume for analysis, 2) reported sample concentrations outside a linear calibration range, and 3) samples below the detection limit.
6. A log page to describe any modifications to the database along with the date of the modification and the user.
7. A verification box for sample receipt and data QA/QC.

The file is called RadFLEx_Compiled_Database.xls and an electronic copy is provided with this report.

pH and DO measurements

The pH measurements of the lysimeter effluent for the quarterly sampling events ranged from 3.32-8.31 with an average of 5.12 and standard deviation of 0.65. This average of 5.12 is near the measured pH of the soil of 5.27 reported in Table 3.1. In all cases the lysimeter effluent sampling events are described using the sample ID representing the date on which the sample was collected. Figure 5.1 shows the measured pH values of each of the lysimeters for all sampling events to date. The average, maximum, and minimum pH values are also shown with the solid black and dashed lines. There were also fluctuations in values during each of the sampling events with the

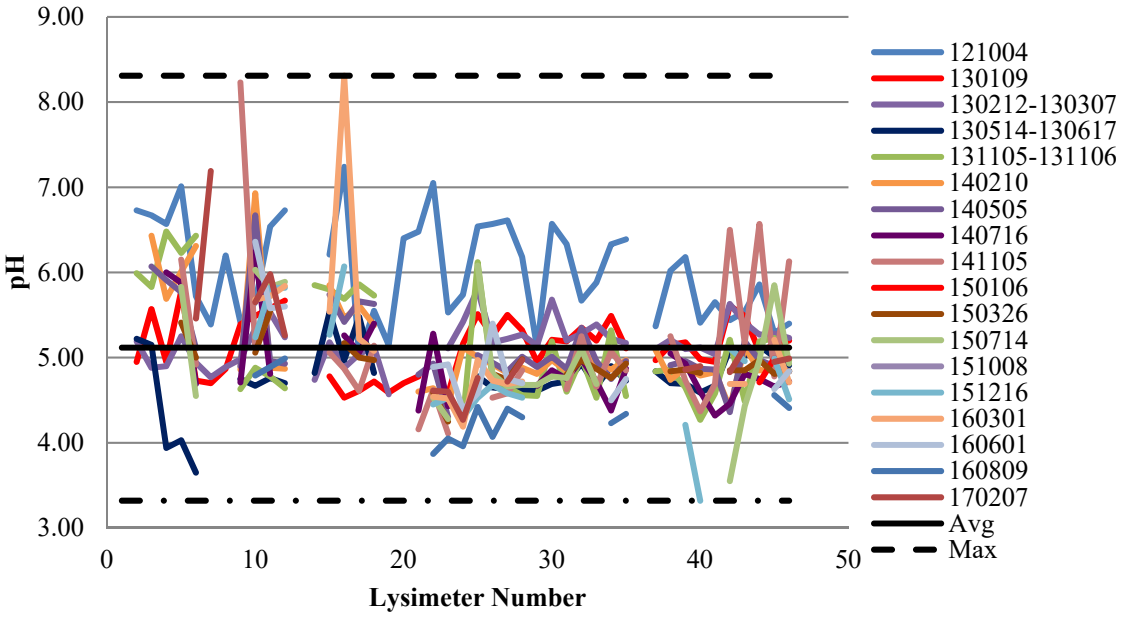

Figure 5.1: The measured pH values of the effluent from each of the lysimeters for all sampling events to date. The average, maximum and minimum of all of the pH measurements are also shown by the solid and dashed black lines.

highest values observed during the 160301 sampling events. This may be due to the shorter sample collection time which did not allow sufficient time for the leachate to reach equilibrium with the soil. Also, several measurements from the 130514-130617 sampling event (lysimeters 4, 5, and 6) appear anomalous with values between pH 3 and 4. However, the effluent from subsequent events is near the average pH of all samples of 5.14.

The observed variability in the pH measurements is important for the overall understanding of these systems. The same soil was used in each of the lysimeters and each are exposed to similar conditions(i.e. temperature and relative amount of rainfall, yet there were as high as 4 pH unit differences). Additionally, there is no trend in the pH of the effluent from the lysimeters containing the cement and saltstone sources. The portlandite (calcium hydroxide, $Ca(OH)_2$) and calcite (calcium carbonate, $CaCO_3$) in the cement will leach when in contact with water and can influence the pH of the surrounding environment but no evidence of this mechanism has been observed. Transport of the radionuclides in this study is greatly affected by pH. Thus, in lysimeters with the same sources, pH variability may help to explain any potential differences in breakthrough. However, it does appear that the average pH of the lysimeters is approaching a constant value of approximately pH 5, which is most likely due to the equilibrium reached between the leachate and the pH ~5 soil used to pack the lysimeters. The average of the pH measurements of all the effluents for each sampling event is shown in Figure 5.2. The convergence to a pH of approximately 5 is consistent with the pH of sediment at the SRS (Powell et al., 2014 and Kaplan et al., 2004).

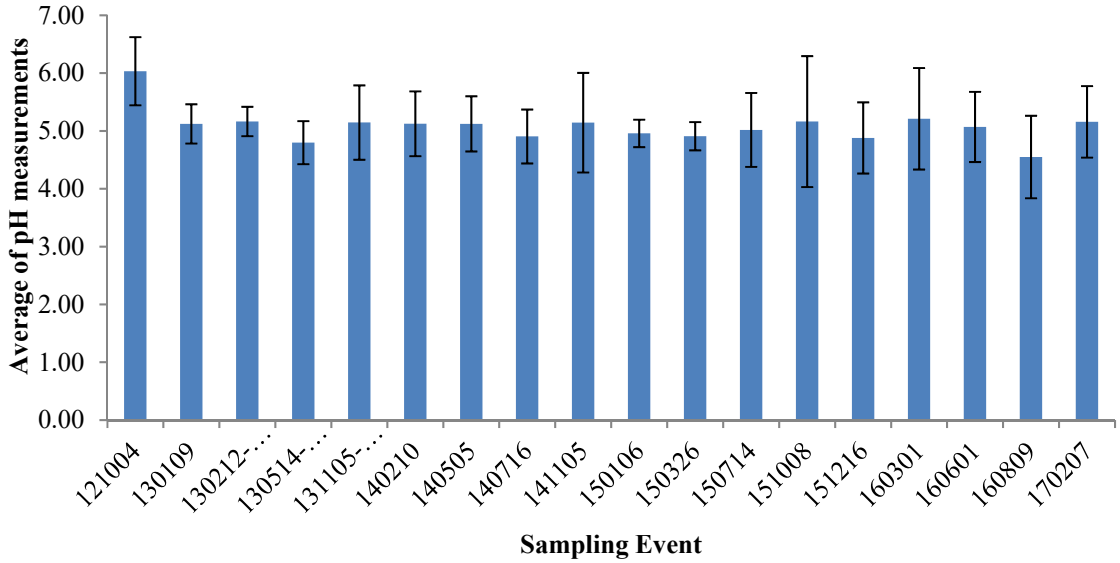

Figure 5.2: The average of the pH values measured for each of the lysimeters during each sampling event.

The DO content of the lysimeter effluent had less variability relative to the pH measurements. The DO content of water in equilibrium with air is dependent on temperature, with increased temperature corresponding to decreased DO content. DO measurements were made as quickly as possible upon receipt of samples so that the measurement most accurately represented the sample when it was collected, and that additional interaction with the environment were at a minimum. Because no attempt was made during sampling and shipment to preserve the *in situ* DO content in these samples, it is expected that the values reported here have been further oxidized, and as such do not necessarily represent the *in situ* values. Figure 5.3 shows the measured DO content in mg L^{-1} of all the effluent samples from all sampling events to date. It is noteworthy that the majority of effluent samples are close to the theoretical saturation value of 8 mg L^{-1} DO. The fall and winter samples were collected during the period of lowest temperature and thus it is surprising that they have the lowest average DO content. With the available

data, an explanation for these low measurements cannot be developed. It will be important to note whether this is an anomaly or whether this in an indication of a shift in the average DO content of these systems when continuing with the measurements in 2016 and beyond. Any large fluctuations in values will also be important to note as they may have an impact on the transport of the radionuclides in the lysimeters. The additional sampling events in 2015 and 2016 indicate that the samples have returned to approximately oxygen saturated conditions and that the low measurements of during event 140210 appear to be an anomaly. With the exception of measured values of 5.7 and 6.1 for lysimeters 35 and 47, respectively, the measured values for the most recent lysimeters are near oxygen saturated conditions.

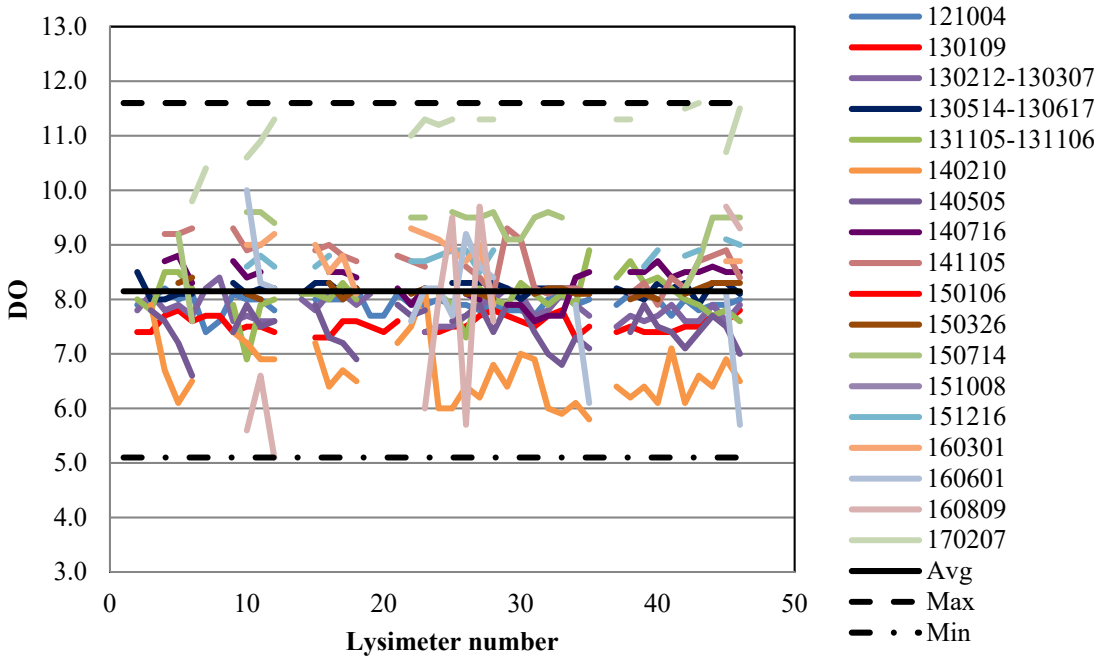

Figure 5.3:The measured DO values (mgL^{-1}) of the effluent from each of the lysimeters for all sampling events to date. The average, maximum and minimum of all of the DO measurements are also shown by the solid and dashed black lines.

Effluent Measurements

Gamma suite radionuclides - ^{60}Co, ^{137}Cs, ^{133}Ba, ^{152}Eu

Nine lysimeters (4-6, 16-18, and 26-28) contained sources consisting of the gamma emitting radionuclides ^{60}Co, ^{137}Cs, ^{133}Ba, and ^{152}Eu. Lysimeters 4-6 contained the nuclides within a cement matrix without additional blast furnace slag (BFS), 16-18 were contained within a saltstone matrix with BFS, and 26-28 were control lysimeters where the nuclides were added directly to a filter and placed in the lysimeters. Of those radionuclides, ^{60}Co was found to have the highest concentrations in the effluent. The measured concentration (Bq L^{-1}) of ^{60}Co from each lysimeter containing the suite of gamma emitting radionuclides for each sampling interval is shown in Figure 5.4. For clarity, Figures 5.5-5.7 contain the data for individual sets (cement, saltstone, and sediment) and the activities for each lysimeter are broken down by sampling event are provided in the RadFLEx database. The concentration of ^{60}Co was greatest in the effluents of lysimeters 4, 5 and 6, which had cumulative releases of 4,185, 8,350, and 3,198 Bq, respectively. Although these concentrations of ^{60}Co are measureable, they still represent a relatively small fraction of the total ^{60}Co in the source as discussed below. In almost all cases, the concentrations of ^{137}Cs, ^{152}Eu, and ^{133}Ba were at or below the minimum detection limit. Thus it appears that only a small fraction of ^{60}Co was initially mobile in these lysimeters. It is clear from sampling events in 2015 and 2016, the measured ^{60}Co was only a small fraction of the otherwise immobile ^{60}Co. However, detailed analysis of the solid phase distribution of ^{60}Co and other gamma emitting radionuclides is needed to verify this.

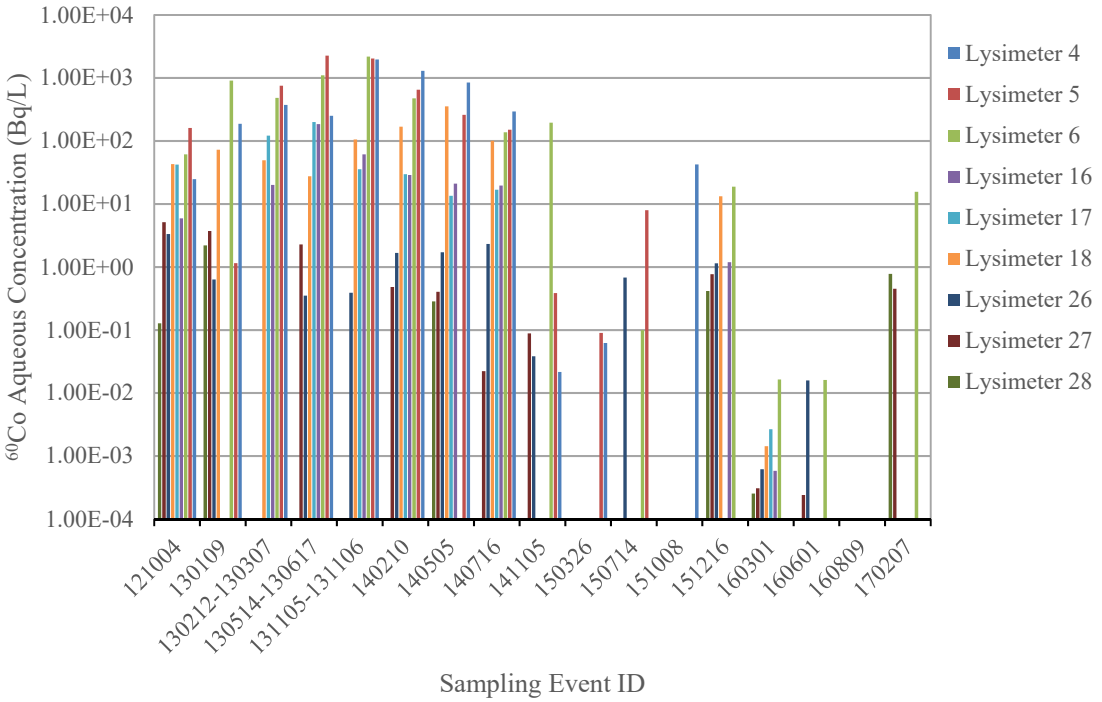

Figure 5.4: Measured activity concentrations (Bq L^{-1}) of ^{60}Co in the effluent of the lysimeters containing gamma emitting radionuclides for each sampling event. Note: samples were not received for the 150106 event.

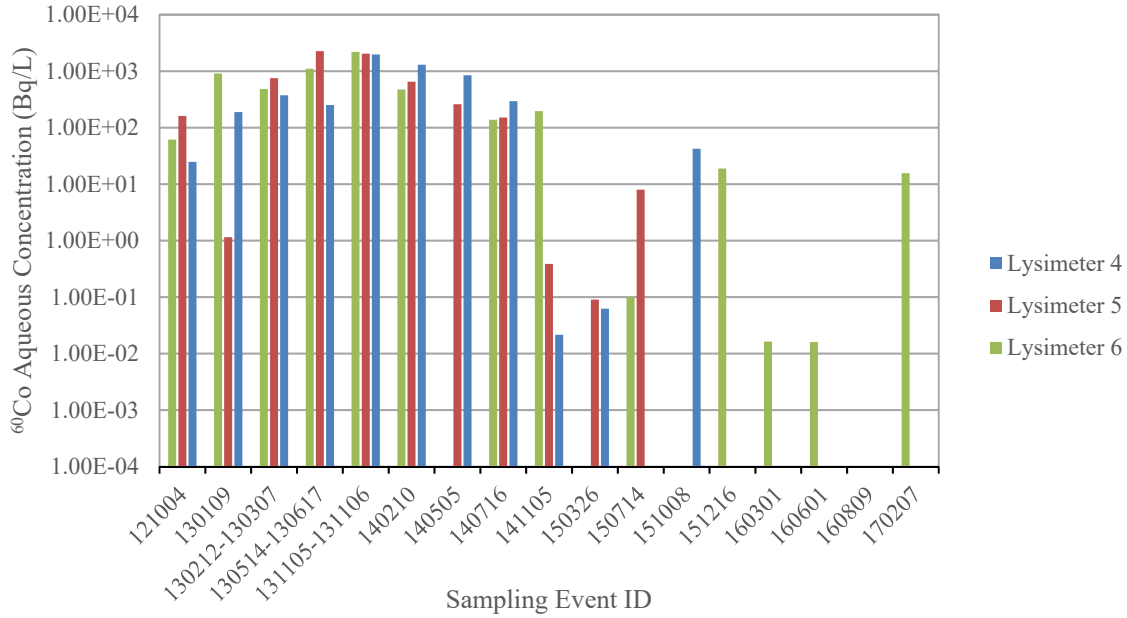

Figure 5.5: Measured activity concentrations (Bq L^{-1}) of ^{60}Co in the effluent of the cement source bearing lysimeters for each sampling event. Note: samples were not received for the 150106 event. To aid in comparison, Figures 5.5-5.7 have similar y-axis values.

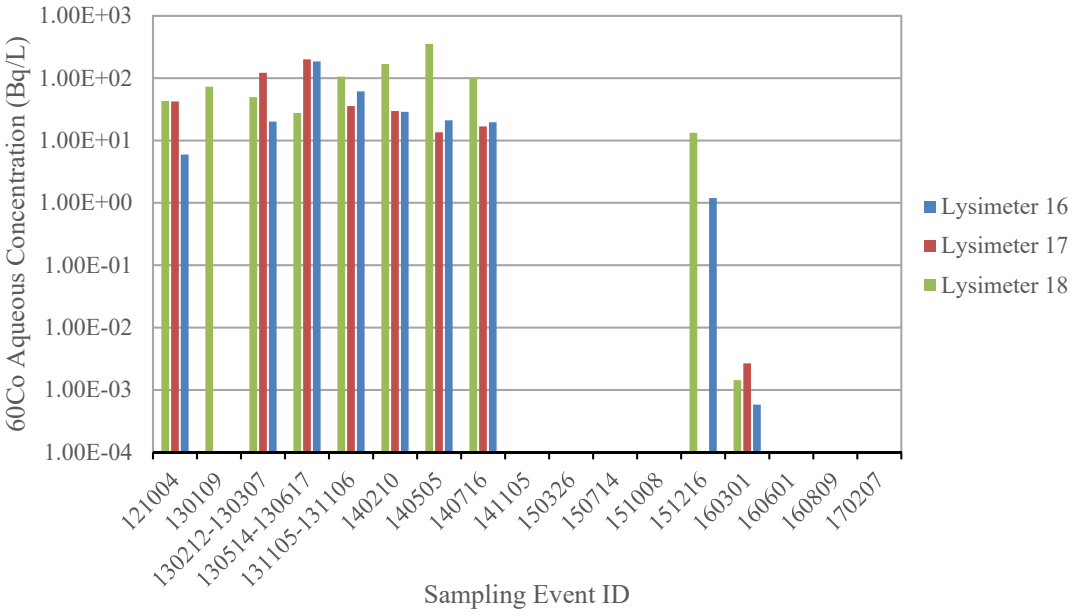

Figure 5.6: Measured activity concentrations (Bq L^{-1}) of ^{60}Co in the effluent of the saltstone source bearing lysimeters for each sampling event. Note: samples were not received for the 150106 event. To aid in comparison, Figures 5.5-5.7 have similar y-axis values.

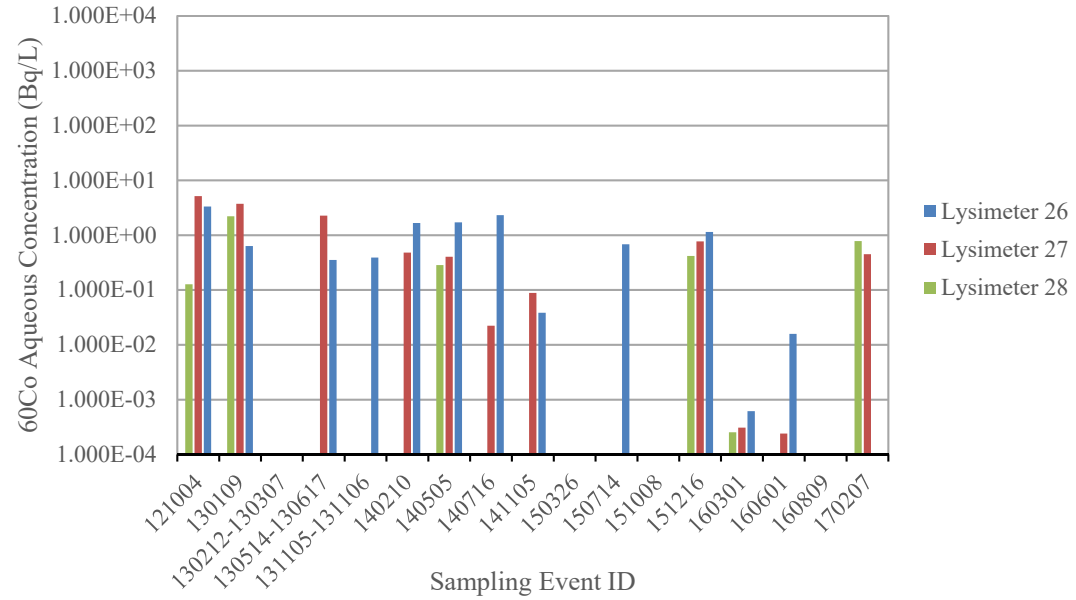

Figure 5.7: Measured activity concentrations (Bq L^{-1}) of ^{60}Co in the effluent of the lysimeters containing only the gamma suite deposited on a filter paper (referred to as the "sediment" source'. Note: samples were not received for the 150106 event. To aid in comparison, Figures 5.5-5.7 have similar y-axis values.

There are several important observations from this data. First, the breakthrough of ^{60}Co from the lysimeters containing the suite of gamma emitters in saltstone sources was approximately an order of magnitude greater from the lysimeters containing cement sources and no BFS. Furthermore, the breakthrough of ^{60}Co from the sediment sources was ~100x lower than that from the saltstone sources and ~10x less than that from the cement sources and no BFS. Thus it appears that the mobilization of ^{60}Co follows the trend:

Saltstone sources > Cement (no BFS) sources > sediment/filter paper

This trend is demonstrated from the compiled data in Table 5.1 which lists the fraction of ^{60}Co released from each lysimeter relative to the total ^{60}Co contained in the source. While the average fraction released is very low for all sources and the standard deviation of the three replicate lysimeters for each source is high relative to the average, it is clear that the lysimeters containing saltstone sources have the highest release of ^{60}Co.

Table 5.1: List of the fraction of ^{60}Co released from lysimeters containing saltstone, cement, and sediment sources.

Lysimeter	Source	Cumulative Effluent Volume (mL)	Total activity in source (kBq)	Cumulative activity released in effluent(kBq)
4	Cement	8246	5106	4.57
5	Cement	11280	5106	8.65
6	Cement	9108	5106	3.27
16	Saltstone	9545	5106	0.53
17	Saltstone	11318	5106	0.72
18	Saltstone	9213	5106	1.00
26	Soil	11022	318	0.01
27	Soil	21808	318	0.01
28	Soil	17296	318	0.00

The main factor that is likely controlling the variability of breakthrough within the group of cement and saltstone gamma suites is the cumulative volume collected. There is an approximately 2.5 L difference between the maximum and minimum effluent collected in each set of cement bearing lysimeters. The variability may also be an indication of the cementitious sources aging differently. The existence of large pores, fracturing, or cracking occurring as the cement and saltstone sources age and interact with the surrounding soil under variable soil moisture conditions could enhance water infiltration into the interior of the source, thereby promoting radionuclide leaching. The variability may also be an indication of compromises in the integrity of the source.

Another important observation made from this data is the release of Co from lysimeters 26-28 was negligible. Conceptually, it was expected that there would be greater breakthrough from the lysimeters containing the sources with the gamma suite spiked in the soil. It appears from the data that the cement and saltstone are facilitating the transport of Co but it is unclear why this is the case. It will be beneficial to examine both the source and soil column from each of the sets of gamma suite containing lysimeters in order to determine whether there has been release from the source of any of the other radionuclides, and if there has been any fracturing in the source that has facilitated release from the source and subsequent transport.

The breakthrough from the lysimeters containing the suite of gamma emitting radionuclides can be conceptualized using knowledge of the geochemical interactions controlling transport of each radionuclide. One approach for predicting this breakthrough is to use partition coefficients (K_d). K_d is an important parameter that defines the

partitioning of an analyte between the solid and aqueous phases and therefore represent a measure of retarded mobility. Examining the K_d values and controlling surficial interactions of the gamma emitting radionuclides included in the RadFLEx study can help explain the observations in this discussion.

The mobility of monovalent Cs is controlled by sorption and cation exchange interaction between Cs to clay mineral particles in soil (Giannakopoulou et al., 2007). Metal concentration, pH, ionic strength, and temperature influence these interactions (Giannakopoulou et al., 2007). Previous explanation of the valence state and sorption behavior of Co at relevant conditions should be considered in this discussion. Additionally, the partitioning of Co varies with pH, redox conditions, ionic strength and dissolved organic matter content, with sorption to iron and manganese oxides and clay minerals limiting mobility (Kim et al., 2006; Krupka and Serne, 2002). The mobility of Ba is controlled by 1) sorption based on the cation exchange capacity (CEC) of the soil and 2) the solubility of Ba particularly in the presence of sulfate and carbonate which can form insoluble $BaSO_4$(s) and $BaCO_3$(s) phases. Adsorption of Ba, facilitated through the incorporation in clay minerals, will increase with increased soil CEC (Medejon, 2012). Precipitation as witherite ($BaCO_3$) will also limit mobility in the presence of elevated $CaCO_3$ content. Sulfate concentrations will also control Ba mobility due to the formation of the $BaSO_4$, which has a very low solubility. The high sorption affinity (and high K_d) of trivalent Eu to sediment is likely due to its low solubility in natural environments (Krupka and Serne, 2002).

K_d values for the gamma emitting radionuclides are listed in Table 5.2. In the work by Grogan et al. (2010), Cs and Co sorption experiments were performed with sediment from the upper and lower vadose zone, and aquifer zone at the E-Area of the SRS. The values listed in the table were the K_d values calculated from Cs and Co sorption to the lower vadose zone sediment because the soil characteristics of this zone were the most representative of the soil used in these experiments. The K_d value listed for Eu was determined from a study of Eu sorption to a clayey soil from the SRS (Kaplan et al., 2010b). A Ba K_d range of 5 to 50 was reported by Seaman and Chang (2013) when examining Ba sorption to two SRS end member soils and a soil from the Saltstone Disposal Facility. This range is similar to the value of 80 reported by Miller (2010) based on a linear extrapolation between measured sorption distribution coefficients of Sr and Ra. Similar to Ba, Ra and Sr are divalent cations and as shown in Sposito (1989), the sorption affinity for alkaline earth metals will follow the trend of increasing sorption with increasing ionic radii ($Ra^{2+} > Ba^{2+} > Sr^{2+} > Ca^{2+} > Mg^{2+}$).

Therefore, breakthrough from the lysimeters containing the suite of gamma emitting radionuclides would, conceptually, be consistent with the K_d values listed in Table 5.2, where mobility in the system would increase with decreasing K_d values. However, there is one inconsistency with the listed values. Only breakthrough of Co has been measured thus far and it would be expected, based on these values, that Cs breakthrough should have occurred first or at least in greater quantities than Co. Investigations of the soil columns from these lysimeters may provide the necessary data to explain this unexpected phenomenon.

Table 5.2: Sediment:water partition coefficient (K_d) values for the radionuclides in the lysimeters containing the suite of gamma-emitting radionuclides.

Radionuclide	K_d (L kg^{-1})
^{137}Cs	6 (Grogan et al., 2010)
^{60}Co	58 (Grogan et al., 2010)
^{152}Eu	9,021 (Kaplan et al., 2010b)
^{133}Ba	Range 5 to 50* (Seaman and Chang, 2013)

*Range of reported values examining sorption to sand and clay end-member soils and a soil from the Saltstone Disposal Facility.

Actinides ($^{239/240/241}Pu$ and ^{237}Np)

There was no measurable release of ^{239}Pu from the eighteen lysimeters containing plutonium using the straightforward ICP-MS based technique with a detection limit of approximately 1 x 10^{-12} M ^{239}Pu. In an attempt to determine if Pu was in the effluent below this detection limit, an ultra-low level analysis technique was developed to concentrate Pu from larger volumes of effluent and determine the Pu activity using alpha spectroscopy. Measurements of plutonium concentration were performed only on 13 lysimeter effluents including three sampling events (150326, 151216 and 160301). Measurements were only done on samples where the effluent volumes were higher than 1 liter and for the same lysimeters in the time series, when it was possible, in order to evaluate plutonium concentrations over the time.

There was measurable release of $^{239,240}Pu$ for only a few lysimeters (Table 5.3). The concentration obtained is between 9x10^{-13} M and 10^{-15} M with a detection limit around 1 x 10^{-15} and 5 x 10^{-15} M which varied based on the alpha spectrometer used. The uncertainties are between 10 and 20 %. All reported values were at or above detection limits and were near the solubility limits of Pu(IV) (hydr)oxide phases. The uncertainty

values are high due to the extremely low concentrations of Pu measured. However, these are positive results identifying $^{239/240}$Pu in the effluent. Thus, it appears that small concentrations of mobile Pu are breaking through the lysimeters though this mass of Pu represents only a small fraction of the total activity in the source.

The observation of extremely low concentrations of aqueous Pu is consistent with a solubility control as previously observed (Kaplan et al., 2006b; Neck and Kim, 2001; Neck et al., 2007). The low concentrations of Pu in the effluent is also consistent with the currently accepted model that plutonium has limited mobility in the subsurface primarily due to reduction of mobile Pu(V) to immobile Pu(IV) on mineral surfaces (Kaplan et al., 2004). Due to the long time period required for this analysis and the fact that these measurements were outside the planned scope of work for FY16, additional measurements have not been performed. Future measurements will attempt to determine the oxidation state of the mobile Pu phase. Based on the high K_d values of Pu(IV) in SRS soils, it is expected the mobile Pu is present in the soluble pentavalent PuO_2^+ dioxycation (Powell et al., 2014).

Table 5.3: $^{239/240}$Pu concentration in effluent from Pu bearing lysimeters at three sampling intervals.

	150326		151216/151008		160301	
Lysimeter	Measured Pu (M)	Uncertainty (M)	Measured Pu (M)	Uncertainty (M)	Measured Pu (M)	Uncertainty (M)
11	8×10^{-15}	1×10^{-15}	$< 5 \times 10^{-15}$		$< 5 \times 10^{-15}$	
33	9×10^{-13}	2×10^{-13}	$< 1.1 \times 10^{-14}$			
35			8.6×10^{-15}	1×10^{-15}		
39	3.8×10^{-13}	5×10^{-14}				
45			2.6×10^{-14}	4×10^{-15}	1.6×10^{-14}	2×10^{-15}
46	9×10^{-13}	2×10^{-13}				

Four lysimeters contain ^{237}Np sources and there was no measurable release during the first three sampling events. Neptunium breakthrough from lysimeters containing Np(V) sources was first observed during the 130307 sampling event where lysimeter 30 had a release of 146 Bq from the source and 140505 sampling event for lysimeter 29 where 43 Bq was found in the effluent. Plots of the cumulative activity of Np (in Bq) released as a function of the cumulative volume of water through lysimeters 29 and 30 are shown in Figure 5.8. While the fraction of Np released from each lysimeter varies, the aqueous concentrations of Np in the effluent from each lysimeter appear to be approaching a similar value (Figure 5.9). Therefore, it may be that release of Np and transport through the soil is solubility controlled. This hypothesis if further supported by comparison with the Np concentration in the effluent from the less soluble NpO_2 source in lysimeter 32.

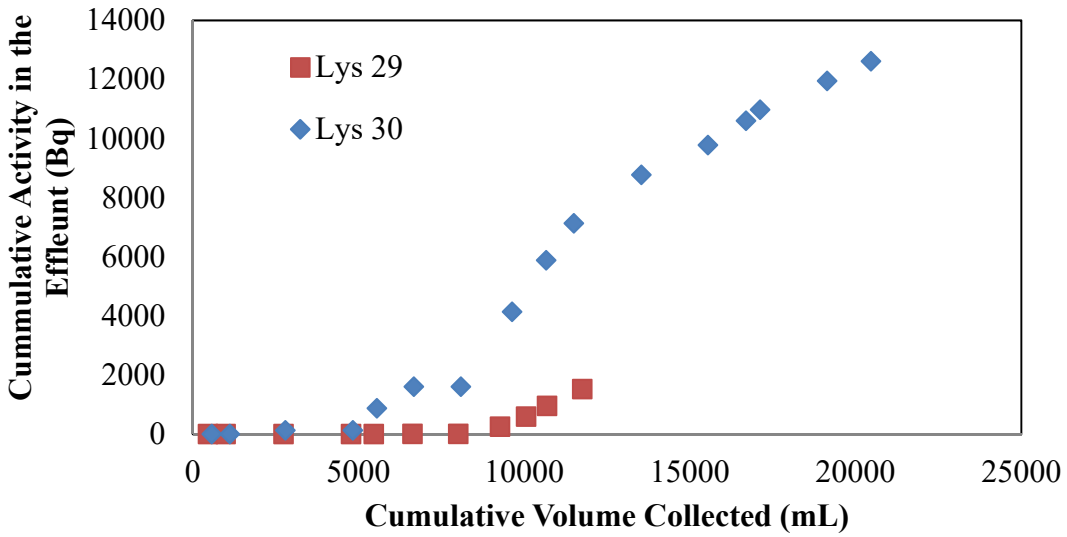

Figure 5.8: The breakthrough of ^{237}Np from lysimeters 29 and 30 shown as the cumulative activity measured in the effluent as a function of cumulative water volume collected.

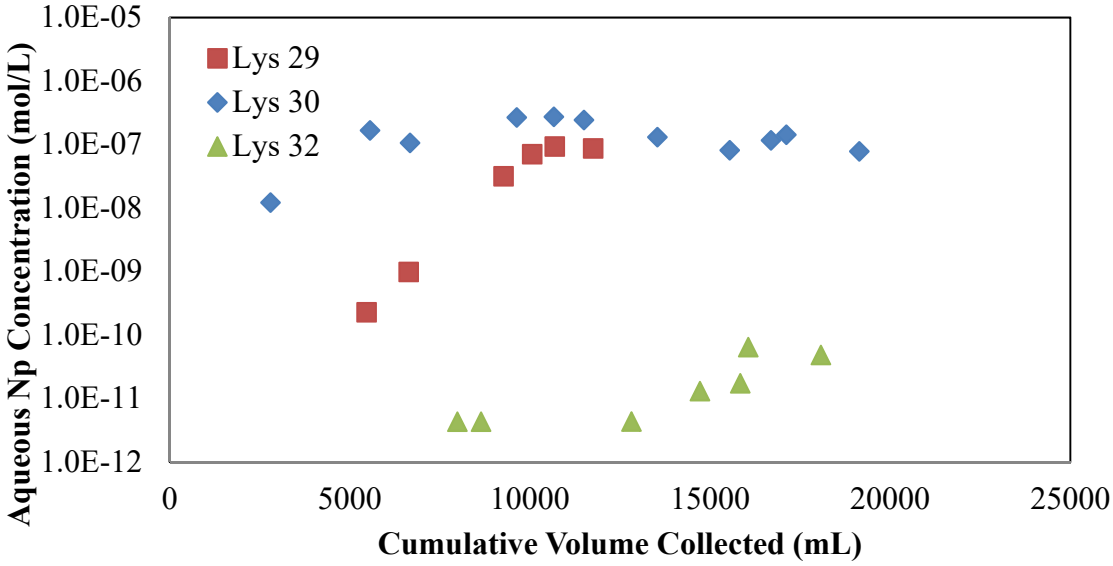

Figure 5.9: The molar concentration of ^{237}Np from lysimeters 29, 30, and 32 shown as the cumulative activity in Bq as a function of cumulative water volume collected.

To date, there has been a total of 12,620 Bq released from lysimeter 30 (Table 5.4) and 1,525 Bq from lysimeter 29 (Table 5.5). Breakthrough from lysimeter 29 was observed during analysis of the 140505 samples.

Breakthrough from the Np(IV) sources, Lysimeters 31 and 32, had not previously been seen. Lysimeter 32 first saw breakthrough in the 141105 sampling, with 0.001 ppb measured in the effluent. All sampling periods from FY15, FY16, and FY17 had measureable Np release as well, with a cumulative activity of 1.05 Bq measured as of FY17 (Table 5.6). Plots of the cumulative activity of Np observed in the effluent as a function of the cumulative volume of water through lysimeter 32 is shown in Figure 5.10. For comparison with the more soluble Np(V) source is lysimeters 29 and 30, the aqueous concentration of Np in the effluent from lysimeter 32 is shown in Figure 5.9.

The measurement of Np from the Np(IV) source in lysimeter 32 is likely due to the oxidation of the source material from Np(IV) to Np(V) in the presence of pore water over time. The fraction of the source measured in the effluent is four orders of magnitude lower than the Np(V) sources.

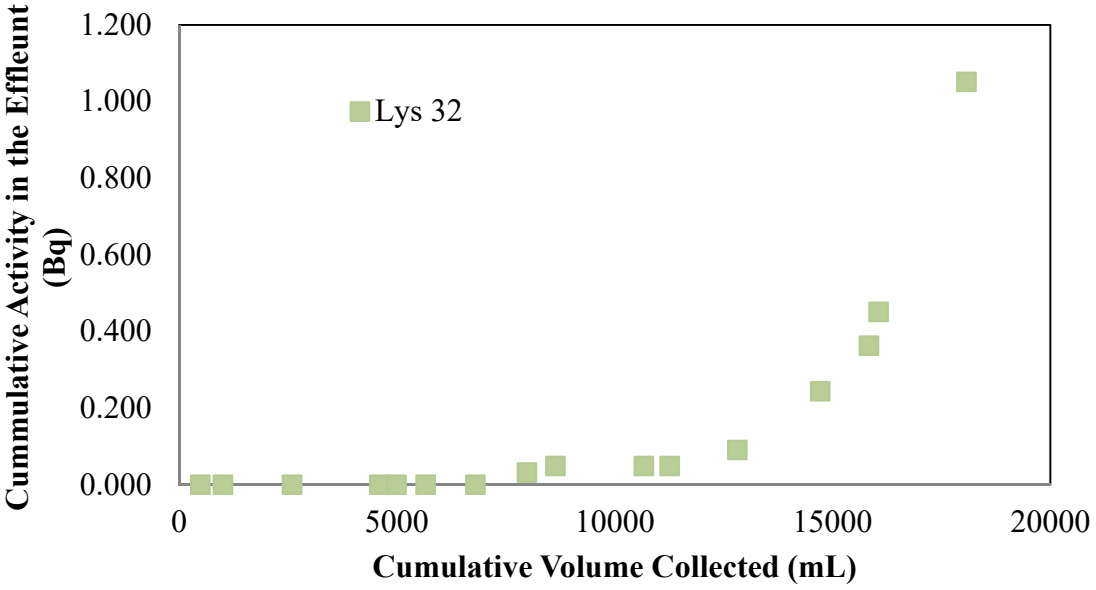

Figure 5.10: The breakthrough of ^{237}Np from lysimeters 32 shown as the cumulative activity measured in the effluent as a function of cumulative water volume collected.

Table 5.4: Cumulative release of ^{237}Np from lysimeter 30. Values in parentheses represent uncertainty.

Sampling Quarter	Cumulative Volume Collected, mL	Measured Np, ug/L	Activity Measured in Effluent, Bq	Cumulative Activity Measured in Effluent, Bq
121004	571.55	0	0.00	0.00
130109	1,116.91	0	0.00	0.00
130212-130307	2,795.62	2.89 (0.01)	126.32 (0.52)	126.32 (0.52)
130514-130617	4,829.33	0	0.00	126.32 (0.52)
131105-131106	5,557.07	39.5 (0.26)	748.14 (4.98)	874.45 (5.01)
140210	6,671.62	25.2 (0.08)	731.09 (2.38)	1605.54 (5.54)
140505	8089.22	0	0.00	1605.54 (5.54)
140716	9631.93	63.10 (0.28)	2534.68 (11.30)	4140.23 (12.59)
141105	10661.64	64.88 (0.26)	1739.79 (6.96)	5880.01 (14.39)
150714	11,498.86	57.51 (0.35)	1253.76 (7.65)	7133.78 (16.29)
151216	13,533.86	30.92 (0.88)	1638.69 (46.88)	8772.47 (49.63)
160301	15,541.86	19.24 (0.014)	1005.91 (0.75)	9778.37 (49.64)
160601	16,691.36	27.54 (0.14)	824.36 (4.11)	10602.73 (49.81)
160809	17,113.86	33.86 (0.29)	372.57 (3.21)	10975.30 (49.91)
170207	19,140.36	18.46 (0.21)	974.14 (10.87)	11949.44 (51.08)
170207-pan**	20,460.87	19.49(0.43)	670.17 (14.95)	12619.61 (53.22)

***Did not receive lysimeter 30 samples for 150106 and 150326**
****Denotes sample received from overflow pan of Lysimeter 30**

Table 5.5: Cumulative release of ^{237}Np from lysimeter 29. Values in parentheses represent uncertainty.

Sampling Quarter	Cumulative Volume Collected, mL	Measured Np, ug/L	Activity Measured in Effluent, Bq	Cumulative Activity Measured in Effluent, Bq
121004	460.1	0	0	0.00
130109	993.19	0	0	0.00
130212-130307	2,739.90	0	0	0.00
130514-130617	4,778.11	0	0	0.00
131105-131106	5,465.30	0.054 (0.0003)	0.97 (0.01)	0.97 (0.01)
140210	6,633.57	0.23 (0.001)	7.10 (0.04)	8.07 (0.04)
140505	8,042.27	0	0	8.07 (0.04)
140716	9,468.98	7.46 (0.07)	244 (2.39)	252 (2.39)
141105	10,260.19	16.63 (0.05)	342 (1.13)	595 (2.64)

150714	10,888.48	22.0 (0.19)	360 (3.17)	955 (4.13)
151008	11,953.48	20.54 (0.587)	570 (16.28)	1,525 (16.80)

Table 5.6: Cumulative release of ^{237}Np from lysimeter 32. Values in parentheses represent uncertainty.

Sampling Quarter	Cumulative Volume Collected, mL	Measured Np, ug/L	Activity Measured in Effluent, Bq	Cumulative Activity Measured in Effluent, Bq
121004	490.45		0	0.00
130109	1,007.88		0	0.00
130307	2,595.09	0	0	0.00
130613	4,596.30		0	0.00
131106	4,993.67	0	0	0.00
140210	5,660.70	0	0	0.00
140505	6,802.37		0	0.00
140716	7,986.08	0.00102 (1x10-4)	0.03(0.01)	0.03 (4.61 x 10-3)
141105	8,640.29	0.00102 (2x10-4)	0.02 (0.0036)	0.05 (5.85 x 10-3)
150326	10,671.29	0	0	0.05 (5.85 x 10-3)
150714	11,260.32	0	0	0.05 (5.85 x 10-3)
151216	12,814.82	0.00103 (2x 10-4)	0.04149 (0.0103)	0.09(1.18 x 10-2)
160301	14,718.32	0.00309 (3x 10-8)	0.15314 (2x 10-6)	0.24 (1.18 x 10-2)
160601	15,837.32	0.00409 (2x 10-4)	0.1193 (7.85x 10-3)	0.36 (1.42 x 10-2)
160809	16,059.82	0.0152 (2 x 10-3)	0.08805 (1.2x 10-2)	0.45 (1.86 x 10-2)
170207	18,075.82	0.01144 (0)	0.60056 (0)	1.05 (1.86 x 10-2)

The observed mobility from lysimeters 29 and 30 was expected based on the known mobility of Np(V) which will be present as the free ion, NpO_2^+, under these conditions. In the work by Miller (2010), a K_d value of 9.05 L kg^{-1} was experimentally determined for Np sorption to SRS subsurface soil. Based on this K_d value and the K_d values of the gamma emitting radionuclides (Table 5.2) the observed breakthrough of Np was expected. The downward migration of Np is controlled by the wetting and drying periods in the soil, where transport occurs during the wetting period and is temporarily halted during drying. The transport of Np(V) is strongly dependent on pH, and under the

conditions in this experiment Np(V) sorption will not be strong enough to further retard Np mobility during the cyclic periods (Miller, 2010). It is noteworthy that breakthrough from lysimeter 29 occurred after a cumulative volume of 8,042 mL was collected, compared to 4,829 mL collected from lysimeter 30. It is unlikely that there is an additional mechanism that is retarding the migration of Np in lysimeter 29, which provides further evidence of the variability that inherently exists in these experiments. The difference in the effluent activity between lysimeters 29 and 30 is proposed to be due to a heterogeneous flow field of water through the lysimeter. Additional tracer studies and possibly ex situ imaging (x-ray computed tomography) studies of water movement through the lysimeters are needed to verify the degree of heterogeneity.

In the absence of an analysis of the solid phase concentrations of Np in lysimeters 29 and 30, the fraction of Np released from the source can be estimated using the effluent concentration and assuming equilibrium sorption within the column. Using the effluent values from Tables 5.4 and 5.5 as the aqueous concentration in the K_d equation and assuming a K_d value of 20 L/kg, the solid phase concentration of Np can be calculated to be 2.32×10^{-6} mol/kg_{soil} for lysimeter 30 and 1.73×10^{-6} mol/kg_{soil} for lysimeter 29. Multiplying these concentrations by the mass of soil within the lysimeter below the source and subtracting that value and the amount of Np measured in the effluent, it is estimated that 75% and 50% of the Np is remaining in the source of lysimeters 29 and 30, respectively.

The observation of Np in the effluent from lysimeter 32 is an unexpected and interesting finding. The $NpO_2(s)$ source within lysimeter 32 is an insoluble phase which

is expected to have a solubility comparable to that of $PuO_2(s)$ (i.e. ~10^{-14} M). Therefore, it is likely that some fraction of the $NpO_2(s)$ phase has become oxidized and Np(V) is leaching from the source. This hypothesis is based on the observation of Np in the effluent far above the expected solubility of $NpO_2(s)$. However, a detailed characterization of the source material to demonstrate this oxidation is occurring must be done to prove this hypothesis. This would be a valuable study demonstrating the long-term stability of Np(V) and Np(IV) sources.

6. SUMMARY

In this work, the concentrations of radionuclides were measured in effluents from field lysimeters. These measurements are from the first five years of a long-term, multi-year experiment. Highlights from these measurements are:

- The concentrations of Pu in the effluents were below the ICP-MS detection limit for all lysimeters containing Pu sources. An additional radioanalytical technique with a detection limit of approximately 10^{-15} M demonstrated that there was measurable Pu in the effluent which was consistent with the release of Pu being a solubility controlled phenomena. This confirms previous studies demonstrating the relatively low mobility of Pu within SRS soils.
- Lysimeters 29 and 30 containing NpO_2NO_3(s) sources have had measurable effluent concentrations of ^{237}Np corresponding to 1,560 Bq and 12,795 Bq. These values correspond to 3% and 27% of the initial source activity assuming a 45.88 kBq initial source[2]. This is consistent with the higher mobility of pentavalent Np(V) which is the source lysimeters 29 and 30. As in previous years, Np was also observed in the effluent of lysimeter 32 which contains a relatively insoluble NpO_2(s) source. The observation of Np in the effluent from this lysimeter implies

[2] Evaluation of multiple NpO_2(s) sources indicates some variability in the total ^{237}Np content in each source despite a similar level reported by Roberts et al., (2012). The variability is likely due to the difficulty of weighing small aliquots of solid actinide sources within a HEPA filtered glovebox at Savannah River National Laboratory. Thus, a better approach is to compare total activity leached and aqueous concentrations of each radioisotope in the effluent waters to evaluate the potential for solubility control of the aqueous concentration.

that the $NpO_2(s)$ is becoming oxidized and releasing Np(V) which can transport through the lysimeter with a relatively low K_d.

- ^{60}Co was the only gamma emitting radionuclide measured in the effluent. The highest concentrations were observed eluting from the lysimeters containing cement with no added BFS and the second highest concentrations were from saltstone sources. All cement and saltstone lysimeter sources contained higher concentrations of ^{60}Co in the effluent relative to a control with the gamma suite of radionuclides added directly to a filter. However, this could be an artifact of the higher radionuclide concentration in the cement and saltstone lysimeter compared with the filter paper source and overall similar fractions of the source have been released. The majority of the ^{60}Co was released within the first 2 years of the experiment and concentrations are now close to detection limits. It is unclear what is causing this enhanced mobility of a small fraction of ^{60}Co in the cement and saltstone sources.
- The pH and DO values between different lysimeters remains constant. However, there is a large degree of variability in the volume of water passing through each lysimeter. Variations in the local climate above the 4” diameter opening to the lysimeter which could cause some of the observed differences. Tracer experiments demonstrated that the lysimeters have preferential flow paths which could also account for some of the differences in the volumes of water in the effluent.

A. APPENDIX A

Supplemental Materials and Methods

Table A.1: Example Datasheet for Instrument Calibration Documentation for 100412 Sampling Interval

Identification number for linking calibration data to sample measurements (Format: *Month-Year-Labbook Number-Labbook page*, where month and year are month and year of sample receipt from SRS).	11-12-1-2
Date of Sample Receipt from SRS	11/06/2012
Description of ^{152}Eu gamma spectroscopy standard (date of preparation, total activity, total volume, vessel)	11/14/12, 10.03 kBq/L, 45mL, 50mL conical centrifuge tube
Gamma spectrometer ID	HPGe (Model: GC4018, SN: 1933074)
Filename of gamma spectroscopy standard measurement	152Eu_std(HPGE6)_01112013
Filename of gamma spectroscopy background measurement	HPGE6_Background_111212
pH meter calibration slope and pH(0) value	98.1%, pH(0)=1.0233

Table A.2: Example Datalog sheet for Lysimeter 2 – 121004

Lysimeter number	2
Sample ID	121004L2
Date of sample collection at SRS	10/04/2012
Date of sample receipt from SRS	11/06/2012
Date of sample being prepared for analysis by Clemson	11/11/2012
Date of analysis at Clemson	11/11/2012 (pH,DO), 11/16/2012 (HPGe)
ID Number for Instrument Calibration datalog sheet	11-12-1-2

Sample pH:	6.73
Sample Dissolved Oxygen Concentration (mg/L):	7.90
Mass of solution plus bottle (g)	653.11
Mass of solution subtracting average mass of collection bottles (g)	398.82

Estimated volume of solution removed for sample archiving (mL)	-
Archived sample ID:	-

Gamma detector ID used for analysis:	HPGe (Model: GC4018, SN: 1933074)
Gamma spectroscopy sample count filename:	45mL_SRS_100412L2_11162012.CNF

7. REFERENCES

Angus, M.J., and F.P. Glasser. The Chemical Environment in Cement Matrices. Scientific Basis for Nuclear Waste Management IX. Mat Res. Soc. Symp. Proc. **1985**, *50*, 547-556.

Caron, F., and Mankarios, G. Pre-assessment of the Speciation of ^{60}Co, ^{125}Sb, ^{137}Cs and ^{241}Am in a Contaminated Aquifer. *Journ. of Environ. Radioact.* **2004**, *77*, 29-46.

Currie, L. A. Limits for Qualitative Detection and Quantitative Determination – Application to Radiochemistry. *Anal. Chem.*, **1968**, *40(3)*, 586-593.

Choppin, G.R., Aspects of plutonium chemistry. *Radiochim. Acta.* **1983,** *32*, 43-59.

Choppin, G.R., Actinide Speciation in the Environment. *J. of Radioact. and Nuc. Chem.* **2006**, *273*, 695-703.

Cleveland, J.M. *The Chemistry of Plutonium*; American Chemical Society: La Grange Park, Il., **1979**.

Collins, R. N., Kinsela, A. S. The Aqueous Phase Speciation and Chemistry of Cobalt in Terrestrial Environments. *Chemosphere*. **2010**, *79*, 763-771.

Demirkanli, D. I., Molz, F. J., Kaplan, D. I., Fjeld, R. A. A fully transient model for long-term plutonium transport in the Savannah River Site vadose zone: Root water uptake. *Vadose Zone J*. **2008**. *7*, 1099-1103

Demirkanli, D. I., Molz, F. J., Kaplan, D. I., Fjeld, R. A.: Soil-Root Interactions Controlling Upward Plutonium Transport in Variably Saturated Soils. *Vadose Zone J*. **2009**. *8*, 574-585.

Duckworth, O.W.; Bargar, J.R.; Jarzecki, A.A.; Oyerinde, O.; Spiro, T.G.; Sposito, G. The Exceptionally Stable Cobalt(III)-desferrioxamine B Complex. *Mar. Chem*. **2009**, *113*, 114-122.

Giannakopoulou, F., Haidouti, C., Chronopoulou, A., Gasparatos, D., Sorption behavior of cesium on various soils under different pH levels. *J. of Haz. Materials.* **2007**, *149*, 553-556).

Grogan, K.P., Fjeld, R. A., Kaplan, D. I., DeVol, T. A., Coates, J. T. Distributions of Radionuclide Sorption Coefficients (K_d) in Subsurface Sediments and the Implications for Transport Calculations. *J. of Environ. Radioact,* **2010,** *101,* 847-853.

Kaplan D.I., Powell B.A., Demirkanli D.I., Fjeld R.A., Molz F.J., Serkiz S.M., Coates J.T. Influence of Oxidation States on Plutonium Mobility During Long-Term Transport Through and Unsaturated Subsurface Environment. *Environ. Sci. Technol.* **2004**, *38*, 5053-5058.

Kaplan, D. I., Demirkanli, D. I., Gumpas, L., Powell, B. A., Fjeld, R. A., Molz, F. J., Serkiz, S. M. Eleven-Year Field Study of Pu Migration from Pu III, IV, and VI Sources. *Environ. Sci. Technol.* **2006a**, *40*, 443-448.

Kaplan, D. I., Powell, B. A., Gumapas, L., Coates, J. T., Fjeld, R. A., and Diprete, D. P., Influence of pH on plutonium desorption/solubilization from sediment. *Environ. Sci. Technol.* **2006b**, *40*, 5937-5942.

Kaplan, D.I., Demirkanli, D.I., Molz, F.J., Beals, D.M., Cadieux Jr., J.R., Halverson, J.E. Upward Movement of Plutonium to Surface Sediments During an 11-year Field Study. *J. of Environ. Radioact*. **2010a**, *101*, 338-344.

Kaplan, D. I., Serkiz, S. M., Allison, J. D. Sorption to Sediments in the Presence of Natural Organic Matter: A Laboratory and Modeling Study. *App. Geochem.*, **2010b**, *25*, 224-232.

Kaplan, D. I., Miller, T. J., Diprete, D., Powell, B. A., Long-Term Radiostrontium Interactions and Transport through Sediment. *Environ. Sci. and Tech.* **2014**. 48(15): 8919-8925.

Kaszuba, J. P., Runde, W. H., The Aqueous Geochemistry of Neptunium: Dynamic Control of Soluble Concentrations with Applications to Nuclear Waste. *Envrion. Sci. Technol.* **1999**, *33*, 4427-4433.

Kersting, A.B.; Efurd, D.W.; Finnegan, D.L.; Rokop, D.J.; Smith, D.K.; Thompson, J.L. Migration of Plutonium in Ground Water at the Nevada Test Site. *Nature*. **1999**, *397*, 56-59.

Kim, J. I. Chemical Behavior of Transuraniuc Elements in Natural Aquatic Systems. In "Handbook on the Physics and Chemistry of the Actinides" (A. J. Freeman and C. Keller, eds.). Elsevier Science Publishers B. V., **1986**.

Kim, J. H., Gibb, H. J., Howe, P. D., Sheffer, M., Cobalt and Inorganic Compounds; World Health Organization: Geneva, Switzerland, **2006**.

Knoll, G. F. Radiation Detection and Management 4th Edition; John Wiley and Sons, New York, New York, **2010**.

Krupka, K.M.; Serne, R.J. **2002.** Geochemical Factors Affecting the Behavior of Antimony, Cobalt, Europium, Technetium, and Uranium in Vadose Sediments. Prepared for CH2M Hill Hanford Group Inc., and the U.S. Department of Energy. DE-AC06-76RL01830.

Lukens, W. W., Bucher, J. J., Shuh, D. K., Edelstein, N.M. Evolution of Technetium Speciation in Reducing Grout. *Environ. Sci. Technol.* **2005**, 39(20), 8064–8070.

Madejon, P. Barium. In *Heavy Metals in Soils: Trace Metals and Metalloids in Soils and their Bioavailability*; Alloway, Brian J., Ed.; Springer, **2012**; pp 507 – 514.

Miller, T., Conceptual Model Testing and Development for Neptunium and Radium Sorption to SRS Sediments. Master's Thesis. Clemson University, Clemson, SC, **2010**.

Molz, F., Demirkanli, I., Thompson, S., Kaplan, D. I., Powell, B. A., *Plutonium Transport in Soil and Plants: An Interdisciplinary Study Motivated by Lysimeter Experiments at the Savannah River Site;* American Geophysical Union Books, in press, **2014**.

National Nuclear Data Center, Brookhaven National Laboratory. http://www.nndc.bnl.gov/chart/ (Accessed July 26, 2014).

Neck, V. & Kim, J. I. Solubility and hydrolysis of tetravalent actinides. *Radiochimica Acta* **2001**, *89*, 1-16.

Neck, V., Altmaier, M., Seibert, A., Yun, J. I., Marquardt, C. M., and Fanghanel, T. Solubility and redox reactions of Pu(IV) hydrous oxide: Evidence for the formation of PuO_2+x(s, hyd). *Radiochimica Acta* **2007**, *95,* 193-207.

Powell, B. A., Kaplan, D. I., Serkiz, S. M., Coates, J. D., Fjeld, R. A. Pu(V) transport through Savannah River Site soils - an evaluation of a conceptual model of surface- mediated reduction to Pu (IV). *J. of Environ. Radioact.* **2014**, *131*, 47-56.

Roberts, K. A., and Kaplan, D. I. Reduction Capacity of Saltstone and Saltstone Components. **2009.** Savannah River National Laboratory, Aiken, SC. SRNL-STI-2009-00637.

Roberts, K. A., Kaplan, D. I., Powell, B. A., Bagwell, L., Almond, P., Emerson, H., Hixon, A., Jablonski, J., Buchannan, C., Waterhouse, Tyler. **2012**. SRNL Radionuclide Field Lysimeter Experiment: Baseline Construction and Implementation. Savannah River National Laboratory, Aiken, SC. SRNL-STI-2012-00603.

Robertson, D.E.; Schilk, A.J.; Abel, K.H.; Lepel, E.A.; Thomas, C.W.; Pratt, S.L.; Cooper, E.L.; Hartwig, P.; Killey, R.W.D. Chemical Speciation of Radionuclides Migrating in Groundwaters. *J. Radioanal. Nucl. Chem.* **1995**, *194*, 237-252.

Santschi, P. H., Roberts, K. A., and Guo, L. D. Organic mature of colloidal actinides transported in surface water environments. *Environ. Sci. Technol.* **2002**, 36, 3711-3719.

Seaman J., and Chang, Hyuk-chik, **2013**. Impact of Cementitious Material Leachate on Contaminant Partitioning. Savannah River Ecology Laboratory. SREL Doc. R-13-0004

Sposito, G. *The Chemistry of Soil.* Oxford University Press: New York, New York, **1989**.

Thompson, S. W., Molz, F. J., Fjeld, R. A., Kaplan, D. I. Uptake, distribution, and velocity of organically complexed plutonium in corn (Zea mays). *J. of Environ. Radioact.* **2012,** 112, 133-140.

Zimmerman, T., Zavarin, M., and Powell, B. A. Influence of humic acid on plutonium sorption to gibbsite: Determination of Pu-humic acid complexation constants and ternary sorption studies. *Radiochimica Acta* **2014**, 102, 629-643.